Management of Bridges Considering Aging Mechanisms and Extreme Events

Final Report
February 2019

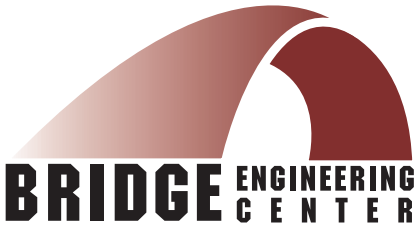

Sponsored by

Midwest Transportation Center

U.S. Department of Transportation
Office of the Assistant Secretary for
Research and Technology

IOWA STATE UNIVERSITY
Institute for Transportation

About the BEC

The mission of the Bridge Engineering Center (BEC), which is part of the Institute for Transportation (InTrans) at Iowa State University, is to conduct research on bridge technologies to help bridge designers/owners design, build, and maintain long-lasting bridges. The mission of InTrans is to develop and implement innovative methods, materials, and technologies for improving transportation efficiency, safety, reliability, and sustainability while improving the learning environment of students, faculty, and staff in transportation-related fields.

About MTC

The Midwest Transportation Center (MTC) is a regional University Transportation Center (UTC) sponsored by the U.S. Department of Transportation Office of the Assistant Secretary for Research and Technology (USDOT/OST-R). The mission of the UTC program is to advance U.S. technology and expertise in the many disciplines comprising transportation through the mechanisms of education, research, and technology transfer at university-based centers of excellence. Iowa State University, through its Institute for Transportation (InTrans), is the MTC lead institution.

About InTrans

The mission of the Institute for Transportation (InTrans) at Iowa State University is to develop and implement innovative methods, materials, and technologies for improving transportation efficiency, safety, reliability, and sustainability while improving the learning environment of students, faculty, and staff in transportation-related fields.

ISU Non-Discrimination Statement

Iowa State University does not discriminate on the basis of race, color, age, ethnicity, religion, national origin, pregnancy, sexual orientation, gender identity, genetic information, sex, marital status, disability, or status as a U.S. veteran. Inquiries regarding non-discrimination policies may be directed to Office of Equal Opportunity, 3410 Beardshear Hall, 515 Morrill Road, Ames, Iowa 50011, Tel. 515-294-7612, Hotline: 515-294-1222, email eooffice@iastate.edu.

Notice

The contents of this report reflect the views of the authors, who are responsible for the facts and the accuracy of the information presented herein. The opinions, findings and conclusions expressed in this publication are those of the authors and not necessarily those of the sponsors.

This document is disseminated under the sponsorship of the U.S. DOT UTC program in the interest of information exchange. The U.S. Government assumes no liability for the use of the information contained in this document. This report does not constitute a standard, specification, or regulation.

The U.S. Government does not endorse products or manufacturers. If trademarks or manufacturers' names appear in this report, it is only because they are considered essential to the objective of the document.

Quality Assurance Statement

The Federal Highway Administration (FHWA) provides high-quality information to serve Government, industry, and the public in a manner that promotes public understanding. Standards and policies are used to ensure and maximize the quality, objectivity, utility, and integrity of its information. The FHWA periodically reviews quality issues and adjusts its programs and processes to ensure continuous quality improvement.

Technical Report Documentation Page

1. Report No.	2. Government Accession No.	3. Recipient's Catalog No.

4. Title and Subtitle	5. Report Date
Management of Bridges Considering Aging Mechanisms and Extreme Events	February 2019
	6. Performing Organization Code

7. Author(s)	8. Performing Organization Report No.
Behrouz Shafei, Dena Khatami, and Shahin Hajilar	

9. Performing Organization Name and Address	10. Work Unit No. (TRAIS)
Institute for Transportation Iowa State University 2711 South Loop Drive, Suite 4700 Ames, IA 50010-8664	**11. Contract or Grant No.** Part of DTRT13-G-UTC37

12. Sponsoring Organization Name and Address		13. Type of Report and Period Covered
Midwest Transportation Center 2711 S. Loop Drive, Suite 4700 Ames, IA 50010-8664	U.S. Department of Transportation Office of the Assistant Secretary for Research and Technology 1200 New Jersey Avenue, SE Washington, DC 20590	Final Report **14. Sponsoring Agency Code**

15. Supplementary Notes

Visit www.intrans.iastate.edu for color pdfs of this and other research reports.

16. Abstract

Current bridge management systems predict the condition state of bridge elements primarily based on the extent of continuous structural deterioration. While the existing systems deliver a range of capabilities for the management of bridges under normal operational conditions, they lack the capability to take into account the consequences of sudden extreme events in a systematic way. In addition to extreme events, the consequences of extreme environmental exposure due to climate change are missing from current management systems. Given the uncertainties involved in natural and manmade hazards in addition to the ones associated with environmental exposure conditions, there is a critical need to develop risk-based approaches that not only take into account the site-specific aging mechanisms and extreme events at the same time, but also accommodate the spatial and temporal randomness originating from these factors. Another significant source of randomness and uncertainty is inspectors' judgment, which directly affects predictions of the condition state of deteriorating bridges. Towards this goal, the current study introduces a risk-based life-cycle cost analysis framework that can be implemented in the current bridge management systems used by transportation agencies.

17. Key Words	18. Distribution Statement
aging mechanism—bridge management—cellular automaton—deterioration—extreme events—finite element—human judgment—life-cycle cost—Markov process—risk	No restrictions.

19. Security Classification (of this report)	20. Security Classification (of this page)	21. No. of Pages	22. Price
Unclassified.	Unclassified.	59	NA

Form DOT F 1700.7 (8-72) **Reproduction of completed page authorized**

MANAGEMENT OF BRIDGES CONSIDERING AGING MECHANISMS AND EXTREME EVENTS

Final Report
February 2019

Principal Investigator
Behrouz Shafei, Assistant Professor
Department of Civil, Construction, and Environmental Engineering
Bridge Engineering Center, Iowa State University

Research Assistants
Dena Khatami and Shahin Hajilar

Authors
Behrouz Shafei, Dena Khatami, and Shahin Hajilar

Sponsored by
Midwest Transportation Center and
U.S. Department of Transportation
Office of the Assistant Secretary for Research and Technology

A report from
Institute for Transportation
Iowa State University
2711 South Loop Drive, Suite 4700
Ames, IA 50010-8664
Phone: 515-294-8103 / Fax: 515-294-0467
www.intrans.iastate.edu

TABLE OF CONTENTS

LIST OF FIGURES

LIST OF TABLES

ACKNOWLEDGMENTS

This report is based on the work supported by the Midwest Transportation Center (MTC). The authors would like to thank the MTC and the U.S. Department of Transportation Office of the Assistant Secretary for Research and Technology for sponsoring this research.

EXECUTIVE SUMMARY

A large number of reinforced concrete (RC) bridges located in the US are at least 50 years old and during their service life are exposed to environmental stressors, operational stressors, and extreme events. Among various sources of deterioration, chloride penetration has major degrading effects on the durability of structures and can potentially make them vulnerable to natural and manmade hazards. To predict the future structural condition of bridges and plan for necessary maintenance and repair actions, the first step is to understand chloride penetration into concrete and then to identify the most influential parameters.

The current study models time-dependent chloride penetration using a comprehensive finite element (FE) model as well as an evolutionary cellular automaton (CA) framework. Through a sensitivity analysis, the contributions and effects of various environmental factors on the chloride profile are investigated in detail. Moreover, the variation of environmental parameters such as temperature, relative humidity, and precipitation due to the effects of climate change and their impact on the performance of bridges is investigated.

Reports on the extent of deterioration due to site-specific stressors, however, greatly depend on the judgment of individual inspectors. Considering the fact that inspection reports are one of the main references in planning for future maintenance activities, it is critical to quantify the effects of the human judgment factor on the prediction of the condition state of deteriorating structures.

Since the errors and deviations originating from this factor may affect the entire life-cycle performance and cost analyses, the current study presents a stochastic approach to systematically investigate the condition-based maintenance strategies under human judgment uncertainties. For this purpose, the thinking process of inspectors is modeled within a probabilistic framework using Brunswikian theory and a probabilistic mental model. A Markov decision process is then utilized to model the deterioration process considering a range of exposure conditions. The deterioration states of the structures under investigation are categorized into five ranks, and the corresponding transition matrices are determined based on an exponential hazard model. By introducing a set of inspection intervals and maintenance criteria, the operational life-cycle cost is estimated by taking into account various confidence levels for the inspection reports.

Current bridge management systems predict the condition state of bridge elements primarily based on the extent of continuous structural deterioration. While the existing systems deliver a range of capabilities for the management of bridges under normal operational conditions, they lack the capability to take into account the consequences of sudden extreme events in a systematic way. Given the uncertainties involved in natural and manmade hazards in addition to the ones associated with environmental exposure conditions, there is a critical need to develop risk-based approaches that not only take into account the site-specific aging mechanisms and extreme events at the same time, but also accommodate the spatial and temporal randomness originating from these factors. Towards this goal, the current study introduces a risk-based life-cycle cost analysis framework that can be implemented in the current bridge management systems used by transportation agencies.

To demonstrate the capabilities of this framework, a set of representative bridges exposed to environmental stressors and seismic hazard risks are investigated. The condition states of the bridges are predicted based on Markovian transition matrices that are generated for both aging mechanisms and seismic events.

CHAPTER 1. INTRODUCTION

1.1. Background

Transportation agencies throughout the United States use various bridge management systems (BMS) to collect and process an array of bridge data for the purpose of predicting the future condition of existing bridges. The outcome is then used to plan appropriate management strategies for the expected service life of bridges. For this purpose, both preventive and corrective actions are essential because the traffic demand increases every year and the bridge components are exposed to the risk of failure due to deterioration processes (i.e., aging mechanisms) from one side and extreme events from the other side.

To systematically investigate the most efficient maintenance efforts, various bridge authorities initiated the development of bridge management systems in the 1980s. The steady progress of these systems resulted in Pontis, which was introduced in the early 1990s with support from the Federal Highway Administration (FHWA). Pontis, which is now known as AASHTOWare Bridge Management software (BrM), is a BMS that performs a variety of functions, such as recording bridge inventory and inspection data, simulating condition states, suggesting possible actions, and developing preservation and rehabilitation policies. Additionally, it can provide a procedure for the allocation of resources for the improvement of multiple bridges in a network. The use of BrM in the United States, however, is still limited and does not go beyond how the component of "risk" is incorporated into the implemented decision-making algorithms.

Penetration of aggressive agents is one of the main reasons of deterioration of reinforced concrete (RC) bridges due to aging mechanisms. Among various sources of aggressive agents, chloride ions have major degrading effects on the durability of bridges and can potentially make them vulnerable to natural and manmade hazards. The adverse impact of chloride penetration into bridge elements becomes more critical for bridges located in marine and tidal zones or in cold areas where bridges are subjected to deicing salts. To predict the future structural condition of these bridge elements and plan for necessary maintenance and repair actions, the first step is to model the time-dependent chloride penetration into concrete numerically and then to identify the most influential parameters.

As a common feature, all bridge management systems attempt to predict the future condition of infrastructure components and plan for proper maintenance and rehabilitation strategies. This, however, cannot be achieved without a thorough investigation of a large number of contributing factors, most of which are not deterministic and contain uncertainties. To include various sources of uncertainty, Moving Ahead for Progress in the 21st Century Act (MAP-21) requires US transportation agencies to integrate "risk" into their existing asset management plans. Risk management is introduced as "a systematic approach to set the best course of action under uncertainty by identifying, assessing, understanding, acting on, and communicating risk issues" (Berg 2010). Risk management greatly helps transportation agencies anticipate the possible consequences of system failure and develop necessary strategies to maintain the system in an acceptable level of performance during both normal and extreme conditions. Among various sources, transportation agencies must especially consider the risks due to natural hazards, such as

earthquakes, hurricanes, and floods. This is to avoid potential disasters, which may occur "when an extreme geological, meteorological, or hydrological event exceeds the ability of a community to cope with that event" (Lindell and Prater 2003).

1.2. Literature Review

1.2.1. Modeling the Deterioration Process of Bridges

Diffusion of aggressive ions such as chlorides in RC bridges is one of the major causes of deterioration in these structures. The chloride penetration normally results in corrosion initiation and propagation. In the initiation stage, surface chloride ions diffuse through the concrete towards the steel rebars. In the second stage, however, the chlorides accumulated at the rebars exceed a critical level, in which the protective film around the rebars is destroyed and voluminous rust material with less strength compared to steel is generated. Among all the models representing the ingress of chloride ions into concrete, the models that include the diffusion and convection terms are the dominant ones. Such models are also capable of taking into account the effects of both internal (e.g., concrete properties and diffusion characteristic) and external (e.g., ambient temperature and relative humidity) parameters (Alipour et al. 2011 and 2013).

There are a number of studies in the literature that attempt to capture chloride penetration and its impact either numerically or experimentally. Saetta et al. (1993) was one of the first studies that modeled the diffusion of chloride ions in one-dimensional unsaturated concrete considering a range of material and environmental parameters. Xi and Bazant (1999) included binding capacity and chloride diffusivity in a model proposed for the study of chloride penetration in saturated concrete. Martin-Perez et al. (2001) used the finite difference approach and studied the chloride binding effect on chloride profiles. Kong et al. (2002) used Xi and Bazant's (1999) model to conduct a reliability analysis on saturated concrete to investigate the influence of water-to-cement ratio and curing time. Ababneh et al. (2003) modeled chloride diffusion in unsaturated concrete considering both diffusion and convention mechanisms. Han (2007) considered the effect of chloride binding and evaporable water on the diffusion coefficient using a finite element (FE) method. Val and Trapper (2008) used a one-dimensional model for chloride ingress, diffusion, and convection into concrete. Bertolini (2008) examined both carbonation and chloride diffusion in a study of concrete corrosion. El Hassan et al. (2010) investigated the effect of environmental conditions, such as humidity and temperature, on the degradation process. Shafei et al. (2012) proposed a three-dimensional finite element model for chloride penetration and estimated the chloride content by solving four nonlinear time-dependent mechanisms simultaneously. Shafei et al. (2013) and Shafei and Alipour (2015) investigated the uncertainties involved in the corrosion process using large-scale stochastic fields.

There are several internal and external parameters that have an impact on the chloride penetration process. Concrete properties and diffusion characteristic are examples of internal parameters, and ambient temperature and relative humidity are known as external parameters. It is known that the external parameters fluctuate due to the change of season and the geographic location of a structure. However, climate change has a direct effect on the average trends of external parameters by changing the temperature, relative humidity, and precipitation in the long

term. According to reports from the Intergovernmental Panel on Climate Change (IPCC), temperature has an increasing trend due to the emission of greenhouse gases. The IPCC defined emission scenarios according to population, economic condition, and technological change. The fifth IPCC assessment (IPCC 2007) particularly includes more comprehensive emission scenarios compared to the fourth IPCC assessment (IPCC 2014). The emission scenarios in the fifth assessment are expressed by representative concentration pathways (RCPs). Overall, the RCP scenarios are similar to the ones in the fourth assessment. For example, RCP 8.5 is broadly comparable to the A2/A1F1 scenario, RCP 6.0 to B2, and RCP 4.5 to B1. However, there is no equivalent scenario for RCP 2.6.

Incorporating the climate scenarios in the chloride penetration model will help decision makers plan for proper maintenance strategies. There are some studies around the world that have investigated the impact of climate change on structural behavior and response. Yoon et al. (2007) evaluated the effect of CO_2 concentration on the carbonation of concrete under the IS92a emission scenario in Korea. Castro-Borges and Mendoza-Rangel (2010) captured historical data (1961 to 2008) on temperature, relative humidity, and precipitation in Yucatan, Mexico, and studied the chloride profile behavior under climate change. Stewart et al. (2011) investigated the deterioration of structures under three scenarios, A1F1, A1B, and 550 ppm, in the Australian cities of Sydney and Darwin. Stewart et al. (2012) showed that carbonation-induced and chloride-induced damage risks may increase by 16% and 3% by 2100, respectively. The authors suggested that in regions where carbonation or penetration of chlorides govern durability, the concrete cover should be increased by up to 10 mm in the design stage to minimize the effect of climate change. Bastidas-Arteaga and Stewart (2015) studied the impact of climate change on the deterioration of structures in France. They considered two emission scenarios, high and medium, and concluded that the current concrete cover might not be satisfactory. Although the listed studies investigated the impact of climate change on the deterioration of structures, there is limited work available in the literature to investigate the effects of climate change on the durability of bridges in the US. In addition, most of the studies used simplified models of chloride penetration to predict the chloride content profile, which may lead to inaccurate results. Furthermore, the existing studies suggest some adaptations in the design stage of structures in order to prevent the aggressive impacts of climate change; however, these studies have not offered any solutions to update the current maintenance and repair strategies.

1.2.2. Prediction of Deterioration Process of Bridges

Markov chain model is the most common stochastic process used for predicting the future condition of deteriorating structures through the estimation of transition probabilities (Thompson et al. 2000, Wellalage et al. 2014, Bu et al. 2014). Jiang and Sinha (1989) applied the Markov chain technique to estimate the stochastic nature of bridge condition. Gopal and Majidzadeh (1991) recommended using a Markov decision process instead of bridge level of service for the management of highway bridges. Scherer and Glagola (1994) indicated that a Markov decision process is a powerful method for bridge management systems. Morcous et al. (2003) adopted Markov chain models and estimated the transition probabilities of the deterioration of bridges for different environmental conditions. Morcous (2006) showed that the Markov chain model's assumptions are acceptable for predicting the future condition of bridge systems. Bocchini et al. (2013) also modeled the deterioration, maintenance actions, and failure of bridges using Markov

chains. It was concluded that the performance and accuracy of Markov models depend on the reliability of the predicted transition probabilities and the techniques used to estimate them (Wellalage et al. 2014).

The transition probabilities are estimated through different methods, such as the percentage prediction method, the expected value method, Poisson regression, negative binomial regression, ordered probit model, and the random effects model (Mauch and Madanat 2001). Nevertheless, some of the stated methods are not suitable for modeling and managing deteriorating structures because they may require a large amount of data to model the stochastic process (Fu and Devaraj 2008). There are several studies in the literature based on the proposed methods to calculate the transition probabilities. Morcous and Akhnoukh (2006) and Bu et al. (2014) modeled the deterioration of bridges by estimating the Markov transition probabilities through the regression model. Robelin and Madanat (2007) and Morcous (2011) used the percentage prediction method to generate the transition probability matrix for modeling the deterioration of structures. Delisle et al. (2004) and Agrawal et al. (2010) found a Weibull distribution suitable for predicting the deterioration of bridges.

The methods listed above for calculating the transition probabilities suffer from several limitations, which may lead to the poor prediction of the future condition of bridges. Madanat and Ibrahim (1995) mentioned that the linear regression method cannot explicitly capture the effect of different explanatory variables and the presence of an underlying continuous deterioration is neglected. In addition, the linear regression method is significantly affected by any prior maintenance actions, records of which may not be readily available in databases. Moreover, Poisson regression and the ordered probit model have limiting assumptions, such as that the observed condition states are independent and identically distributed (2002). To address this issue, time-dependent deterioration forecasting models are introduced and the Markov transition probabilities are described by hazard models. Mishalani and Madanat (2002) determined the transition probabilities based on a Weibull hazard function. Similar to Mishalani and Madanat (2002), Tsuda et al. (2006) estimated the bridge deterioration process using a hazard model. Contrary to the Mishalani and Madanat (2002) model, the transition probabilities in Tsuda et al. (2006) are independent of the history of deterioration and only consider inspection intervals and hazard rates. Kobayashi et al. (2010) investigated multiple condition states and historical operation times to model the deterioration process using a multi-stage Weibull hazard model.

1.3. Objectives and Report Organization

The objective of this study was to improve current bridge management systems through the following:

1. Incorporating a physics-based model to estimate the deterioration of bridge elements due to aging mechanisms. Two numerical frameworks, FE and cellular automaton (CA), were developed to express the ingress of aggressive ions in three-dimensional (3D) concrete elements. It was revealed that the accuracies of both frameworks are good; however, CA is more efficient in terms of computational cost.

2. Including the uncertainties involved in the environmental stressors. Environmental stressors and their variation have a direct impact on the deterioration process of bridges. It was shown that the variation of environmental parameters such as temperature, relative humidity, and precipitation due to climate change can accelerate the deterioration process.

3. Quantifying the effect of the human judgment factor on the prediction of the condition state of deteriorating structures. For this purpose, the thinking process of inspectors was modeled within a probabilistic framework using Brunswikian theory and a probabilistic mental model. The most appropriate inspection and maintenance activities were identified by factoring human error into the decision-making process.

4. Modeling the simultaneous effects of aging mechanisms and extreme events. It was illustrated that considering the adverse effects of extreme events can contribute to improving the life-cycle performance of bridges and cost prediction in the management of bridges.

The outcomes of this study highlight how incorporating the physics-based model, uncertainties due to climate change, and human error as well as the occurrence and consequences of extreme events can contribute to improving the life-cycle performance of bridges and cost predictions. With these outcomes, stakeholders can better plan for necessary maintenance and repair actions, which can lead to an optimized bridge management system. This report is divided into four chapters. Chapter 2 describes the deterioration process of bridge elements due to aging mechanisms. The physics-based model as well as uncertainties regarding environmental stressors are explained in this chapter. Chapter 3 provides an explanation of how to predict the future condition of bridges using a stochastic process. The effects of both human judgement and extreme events are captured. Finally, Chapter 4 provides conclusions.

CHAPTER 2. CHLORIDE PENETRATION INTO CONCRETE BRIDGE ELEMENTS

2.1. Chloride Penetration

Corrosion of steel rebar is a limiting factor in the durability and performance of RC bridges. The corrosion process starts due to the ingress of chloride ions into the RC structural components. The transport of free chloride in concrete is through diffusion and convection. In the present study, both diffusion and convection are taken into account.

$$\frac{\partial C_{tc}}{\partial t} = \text{div}\left(D_{cl} w_e \vec{\nabla}(C_{fc})\right) + \text{div}\left(D_h w_e C_{fc} \vec{\nabla}(h)\right) \quad (2\text{-}1)$$

The first and second terms in Equation 2-1 determine the diffusion and convection terms, respectively. In Equation 2-1, C_{tc} is the total chloride ion concentration of concrete (kg/m^3), t is the time (s), D_{cl} is the chloride diffusion coefficient (m^2/s), w_e is the evaporable water content (m^3 pore solution/m^3 concrete), C_{fc} is the concentration of free chloride ions (kg/m^3 of pore solution), D_h is the humidity diffusion coefficient (m^2/s), and h is the pore relative humidity. The impact of environmental exposure is reflected in the diffusion coefficient by updating its value at each time step of the simulation as follows:

$$D_{cl} = D_{cl,ref} f_1(T) f_2(t) f_3(h)\, f_4(C_f) \quad (2\text{-}2)$$

where $D_{cl,ref}$ is a reference diffusion coefficient and $f_1(T), f_2(t), f_3(h)$, and $f_4(c_f)$ are modification factors for temperature, aging, humidity, and surface chloride, respectively. The temperature modification factor is applied to both the chloride and humidity diffusion coefficients. This factor is defined according to the Arrhenius law and consists of activation energy, E, and the difference between current temperature (T) and reference temperature (T_{ref}).

$$f_1(T) = \exp\left[E/R(1/T_{ref} - 1/T)\right] \quad (2\text{-}3)$$

The aging modification factor represents the reduction of the diffusion coefficient due to progressive hydration over time and decreasing cement porosity.

$$f_2(t) = (t_{ref}/t)^r \quad (2\text{-}4)$$

This factor is directly proportional to the ratio of the reference time (28 days) and the age of the concrete. In Equation 2-4, r is the empirical age factor, assumed to be equal to 0.04.

The existence of humidity and moisture is necessary for the diffusion process, since water is serving as a transport agent and a chemical reactant. The humidity modification factor is defined as follows:

$$f_3(h) = \frac{1}{[1+[(1-h)/(1-h_c)]^4]} \quad (2\text{-}5)$$

where h_c is the critical humidity level at which $f_3(h)$ equals the average of its maximum and minimum values. Finally, the effect of free chloride content can be expressed as follows:

$$f_4(c_f) = 1 - k(c_f)^n \quad (2\text{-}6)$$

where k and n are empirical parameters, equal to 8.4 and 0.5, respectively.

Since the temperature and humidity vary within a three-dimensional concrete member, it is essential to find the nodal temperature and humidity at different points of the model. The governing partial differential equation for the heat flow can be written as follows:

$$\text{div}(K_t\ grad(T)) + q_t = \rho c_t \frac{\partial T}{\partial t} \quad (2\text{-}7)$$

where K_t, q_t, ρ, and c_t are the thermal conductivity of concrete, the rate of heat generation per unit volume, concrete density, and the specific heat of concrete, respectively.

Moisture in concrete flows from regions where moisture is plentiful to where it is scarce. The moisture flux can be modeled by Fick's second law.

$$\frac{\partial w_e}{\partial t} = \frac{\partial w_e}{\partial h} = \text{div}\left(D_h \overrightarrow{\nabla}(h)\right) \quad (2\text{-}8)$$

where the moisture capacity ($\frac{\partial w_e}{\partial \text{h}}$) is equal to the derivative of free water (w_e) with respect to pore relative humidity (h). For a constant temperature, w_e and h are related by an adsorption isotherm as follows:

$$w_e = \frac{CKV_m h}{(1-kh)[1+(C-1)Kh]} \quad (2\text{-}9)$$

where V_m is the monolayer capacity, C is a constant value that represents the effect of temperature on the adsorption isotherm, and *K* is another constant value (Xi et al. 1994). Similar to the chloride diffusion coefficient, humidity, temperature, and aging factors modify the humidity diffusion coefficient.

$$D_h = D_{h,ref} g_1(h) g_2(T) g_3(t) \quad (2\text{-}10)$$

$$g_1(h) = \alpha_h + \beta_h \left[1 - 2^{-10^{\gamma_h (h-1)}}\right] \quad (2\text{-}11)$$

$$g_2(T) = \exp\left[E/R(1/T_{ref} - 1/T)\right] \quad (2\text{-}12)$$

$$g_3(t) = \chi + (1-\chi)\left(\frac{28}{t}\right)^{0.5} \quad (2\text{-}13)$$

where α_h, β_h, and γ_h are the empirical coefficients. In order to determine the profiles of chloride, humidity, and temperature over time, it is necessary to solve simultaneously the system of partial differential equations of 2-1, 2-7, and 2-8. To this end, numerical methods such as finite element and finite difference can be implemented.

2.2. Influential Parameters

According to previous studies, there are several external and internal parameters that affect chloride penetration into concrete. In the current report, three external parameters and one internal parameter are selected for further investigation. Temperature, humidity, and surface chloride are the external parameters that vary in different locations and seasons. For example, during the wintertime, deicing salts, which are frequently used on roads, introduce a major source of chloride ions to the surface of RC bridges. Among the values reported in the literature, the minimum and maximum of temperature and humidity directly depend on the location of structures. Martin-Perez et al. (2001) captured the annual fluctuations of temperature and humidity using a sinusoidal function. Chen and Mahadevan (2008) defined a similar function with a mean of 15°C and an amplitude of 10°C. Shafei et al. (2012) presented the mean and amplitude of temperature and humidity for the Los Angeles area with sinusoidal functions fitted to the historical data. To study the variation of temperature and humidity as two external parameters and their effects on chloride penetration, their seasonal variation is defined in the current study through a sinusoidal function. The following equations show the time-dependent changes of temperature and humidity:

$$T_{ex}(t) = T_{ex,ave} + a\sin\left(\frac{2\pi t}{365}\right) \quad (2\text{-}14)$$

$$H_{ex}(t) = H_{ex,ave} + b\sin\left(\frac{\pi t}{365}\right) \quad (2\text{-}15)$$

In the current study, three different values are selected for the mean of temperature, $T_{ex,ave}$, and the mean of humidity, $H_{ex,ave}$. $T_{ex,ave}$ is 261, 291, and 321 K, while $H_{ex,ave}$ varies between 0.45 and 0.85 in intervals of 0.20. The listed values represent different exposure conditions and are applied to the generated finite element models as boundary conditions.

The third most important external parameter that has a direct impact on the chloride profile is surface chloride. The source of surface chloride can be either deicing salt in winter or seawater in coastal areas. Therefore, monitoring RC structures in regions with a harsh winter or in tidal zones becomes a critical issue for managing the existing infrastructure components. The surface chloride due to deicing salt can be represented by a step function with a maximum value during cold seasons and zero for the rest of year. There are some studies that capture the surface

chloride concentration. A comparison among them indicates that the RC structures in splash and tidal zones are exposed to a much higher chloride content than structures experiencing deicing chloride. To investigate the variation under different exposure conditions, three surface chloride contents of 1.5, 3.5, and 5.5 kg/m^3 are considered in the current study.

In addition to the external parameters, the chloride diffusion coefficient plays a significant role in chloride penetration. This parameter is sensitive to several factors, such as water-to-cement ratio, curing, concrete mixture (additive), and the age of the structure. A wide range of D_{Cl} values, from 1×10^{-12} m^2/s to 25×10^{-12} m^2/s, is reported in the literature (Dhir et al. 1990, Funahashi 1990, Papadakis et al. 1996, Stewart and Rosowsky 1998, Bamforth 1999, Bentz 2003, Chen and Mahadevan 2008, Val and Trapper 2008). The value assumed for D_{Cl} in the present work is 6.7×10^{-12}. A sensitivity analysis was also performed to investigate the impact of this parameter on the chloride profile over time.

2.3. Computational Methodologies

2.3.1. Finite Element Model

To capture the effects of the main internal and external parameters, a three-dimensional finite element model is generated. As explained earlier, the four mechanisms of heat transfer, moisture transport, carbonation process, and chloride penetration are solved simultaneously at each time step. The obtained results are then used to update the model for the next time step. In the current study, the ANSYS program is used to model the chloride penetration into the RC structures. The elements of choice (Solid 70) have eight nodes with a single degree of freedom for temperature. The finite element models utilized for three exposure scenarios are presented in Figure 2-1.

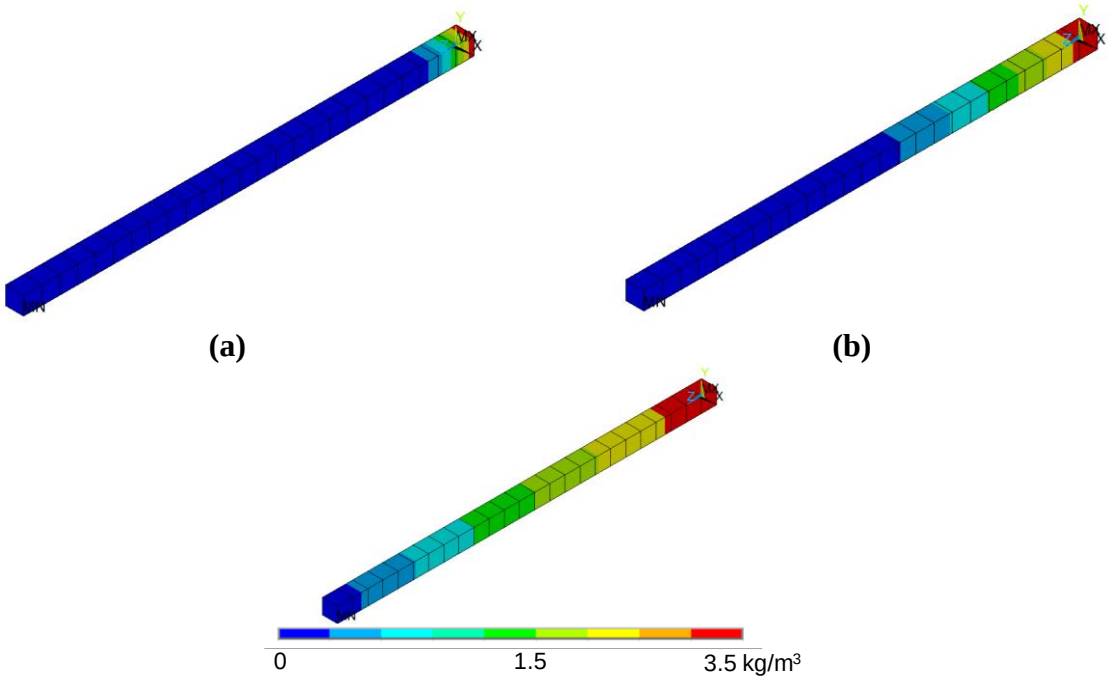

Figure 2-1. Chloride penetration after 60 years under three environmental exposure scenarios: (a) mean temperature 261 K and relative humidity 0.45, (b) mean temperature 291 K and relative humidity 0.65, and (c) mean temperature 321 K and relative humidity 0.85

The concrete element has dimensions of 0.01 × 0.01 × 0.25 m (a typical bridge deck with a unit-length cross section) and is exposed to a chloride concentration of 3.5 kg/m^3 on the top surface. In this figure, the chloride diffusion coefficient is assumed to be equal to 6.7×10^{-12} m^2/s. As can be seen in the figure, after 60 years of exposure, chloride ions reach 24% of the element's length. The FE framework has the capability to define a series of physical environments to investigate the effect of multiple external stressors and provides an accurate prediction of the chloride profile for a concrete element.

2.3.2. Cellular Automata Model

A CA is a lattice-based method in which the evolution of the quantities assigned to each site of the lattice are governed by the laws of physics. In the CA framework, the system under consideration is discretized in space to form lattice sites, each of which are endowed with a finite number of states. Those states evolve during the course of CA simulations in discrete time steps according to the rule of automaton, which updates the states of a certain site at each time step based on the states of that site and its neighbors at the previous time step. The CA method has been successfully employed to model a number of physical phenomena in engineering materials and structures, such as recrystallization, corrosion, hydration, friction, and wear. One of the most interesting applications of CA is the simulation of the diffusion of aggressive agents in

microporous media. In this study, the CA method is adopted to investigate the diffusion of chloride ions in RC structures.

The effectiveness of the CA simulations is greatly dependent on the proper description of the lattice sites' neighborhoods, as well as the correct implementation of the rule of automaton. A lattice site's neighborhood refers to a set of local sites, often called the local environment, which forms the basis for determining the behavior of an automaton. There are two widely used choices to define a local environment in a two-dimensional lattice: von Neuman and Moore. The former environment, shown in Figure 2-2a, consists of a site and the four neighborhood sites nearest to it, while in the latter environment, shown in Figure 2-2b, the next-nearest neighbor sites are also included.

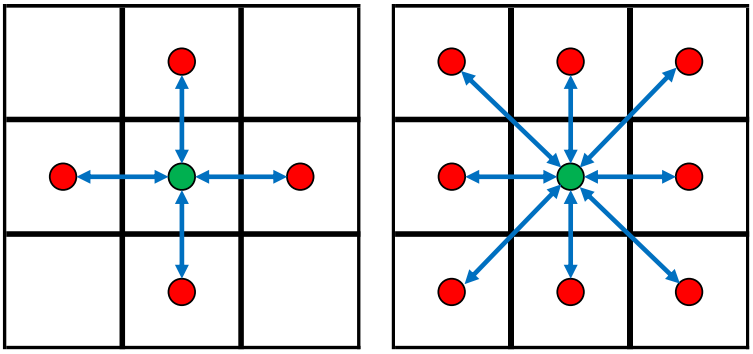

Figure 2-2. Two ways to define a local environment in a two-dimensional lattice: (a) von Neuman and (b) Moore

In these figures, the state of the central cell (green circle) depends on the rule of automaton that involves the neighborhood sites (red circles). The von Neuman environment has been previously used in the literature (Biondini et al. 2004 and 2008). However, it is assumed that the Moore environment yields more accurate results because the additional next-nearest neighborhood sites also contribute to the evolution of the central site, in contrast to the von Neuman environment, in which only the nearest neighborhood sites are involved. To the best of our knowledge, this is the first study that aims at investigating the effect of the local environment (i.e., von Neuman and Moore) on the diffusion of chloride ions in the CA framework.

Once the proper local environment is chosen, the state of each lattice site, i.e., chloride concentration, is updated based on the rule of automaton as follows:

$$C_i(t + \Delta t) = \emptyset_i C_i(t) + \sum_{j=1}^{n} \emptyset_j C_j(t) \qquad (2\text{-}16)$$

where $C_i(t)$ is the concentration of chloride in lattice i measured at time t. The dummy index j refers to the neighborhood lattice sites in the local environment. Thus, n is equivalent to 4 and 8 for the von Neuman and Moore environments, respectively. The coefficients $\emptyset_i$ and $\emptyset_j$ are the so-called order parameters, which vary in space and time to define the local state of the system. To

meet the restrictions due to the conservation of mass principle, the values of the order parameters must satisfy the normality role:

$$\emptyset_i + \sum_{j=1}^{n} \emptyset_j = 1 \quad (2\text{-}17)$$

It should be noted that in isotropic media like RC structures, the order parameters of the neighborhood cells must be equivalent to each other to avoid unrealistic directionality effects. In this study, a constant value of 0.5 is used for the order parameter of the central cell ($Ø_i$), as recommended previously by Biodini et al. (2004 and 2008). To regulate the process according to the constant diffusion coefficient (D), it is vital to discretize space and time such that the cell dimensions (Δx) and time steps (Δt) satisfy Fick's second law, which assumes a linear relationship between mass flux and diffusion gradient. By rearranging the rule of automaton based on the conservation of mass principle, and recalling the differential equations of Fick's second law, it can be easily shown that such regulation yields the following:

$$D = \frac{1-\emptyset_i}{4}\frac{\Delta x^2}{\Delta t} \quad (2\text{-}18)$$

The chloride profile calculated by the CA framework is presented for a typical rectangular cross section of a bridge pier stem subjected to a NaCl aqueous solution around its perimeter. The modeled bridge pier has a width and height of 1.0 and 1.5 m, respectively. The CA grid size is 1 cm, and a von Neuman local environment is assumed. The two-dimensional periodic boundary conditions are applied to the pier's cross section. The diffusion coefficient is assumed to be 6.7×10^{-12} m^2/s, which falls in the range observed experimentally for RC structures exposed to harsh aqueous environments (Hoffman and Weyers 1994, Bentz 2003). This cross section is subjected to a diffusive attack from an aggressive environment along the whole external perimeter with a constant surface chloride concentration of 3.5 kg/m^3. The diffusion process in the pier's cross section for a total life-cycle of 60 years is described by the maps of chloride concentrations shown in Figure 2-3.

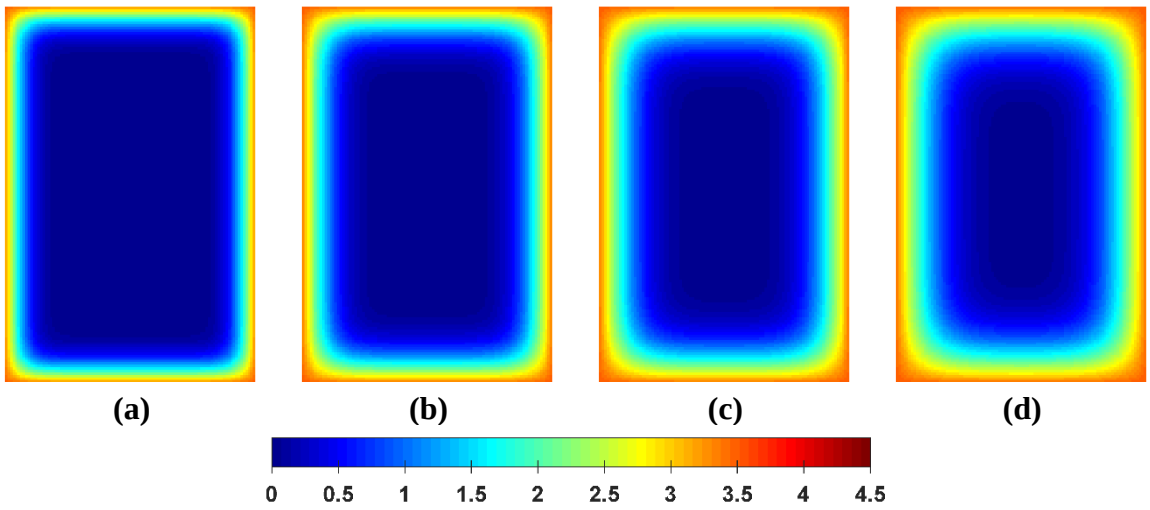

Figure 2-3. Maps of chloride concentrations after (a) 15, (b) 30, (c) 45, and (d) 60 years from the time of diffusion initiation

It can be seen that as the pier ages, the surface chloride diffuses from the perimeter towards the middle of the section. Interestingly, even at the age of 15 years, there is a considerable concentration of chloride that could pass the cover and reach the reinforcing bars.

Both the FE and CA numerical frameworks are capable of modeling the ingress of aggressive agents into the concrete elements. Although FE is one of the most robust computational techniques in the literature, it needs more computational time compared to the CA framework. Therefore, it is suggested that for probabilistic/reliability analyses with several sets of simulations, the CA framework should be implemented; otherwise, both the CA and FE frameworks provide good accuracy and have good agreement with the experimental/field results.

2.4. Results and Discussion

Based on the simulations conducted in this study, it is found that temperature has a direct influence on chloride diffusion. This is because any increase in temperature accelerates the movement of chloride ions. Figure 2-4 shows the impact of temperature on chloride content at the rebar depth (5.0 cm). The relative humidity and surface chloride content are assumed to be equal to 0.65 and 3.5 kg/m^3, respectively.

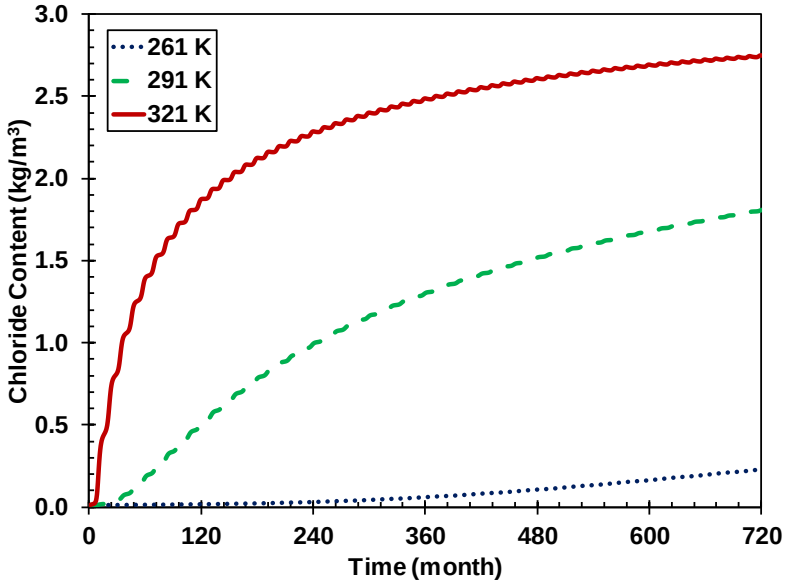

Figure 2-4. Chloride content profile under three different mean temperatures

According to this figure, while the chloride content after 60 years is 0.23 kg/m^3 at 261 K, it increases to 1.80 kg/m^3 at 291 K. If the temperature increases another 30 K (from 291 to 321 K), the chloride content will experience an approximately 50% increase again.

The influence of temperature on the chloride diffusion coefficient is shown in Figure 2-5. The relative humidity and surface chloride content are assumed to be equal to 0.65 and 3.5 kg/m^3, respectively. There is a major difference (up to three orders of magnitudes) among the D_{Cl} values recorded under different temperatures.

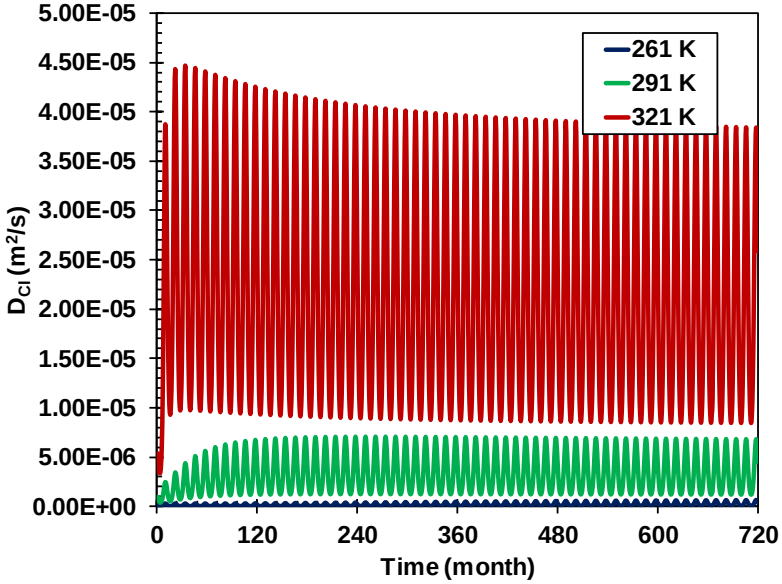

Figure 2-5. Fluctuations of D_{Cl} under three different mean temperatures

Similar to temperature, an increase in humidity leads to a higher chloride content in the concrete mainly because it facilitates the transport of chloride ions. The effects of humidity on chloride profile and D_{Cl} are presented in Figures 2-6 and 2-7, respectively. In both figures, the mean temperature and surface chloride content are assumed to be equal to 291 K and 3.5 kg/m^3, respectively.

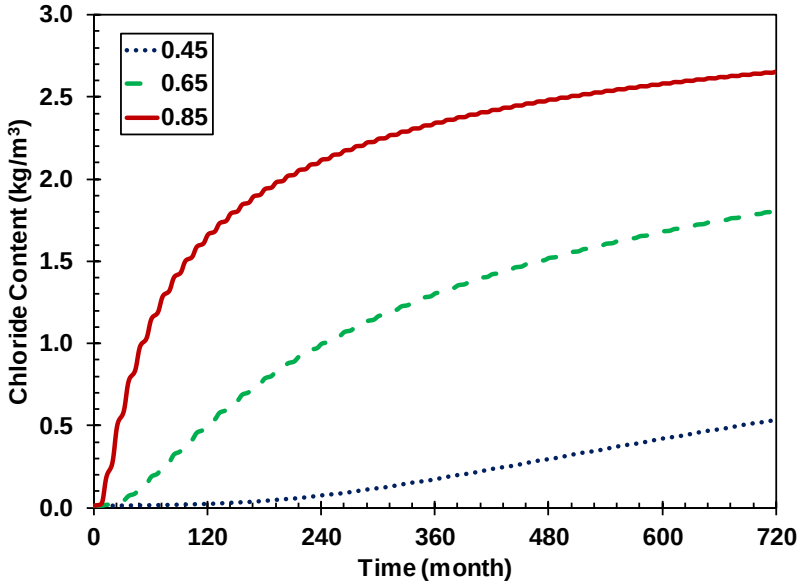

Figure 2-6. Chloride content profile as a function of relative humidity

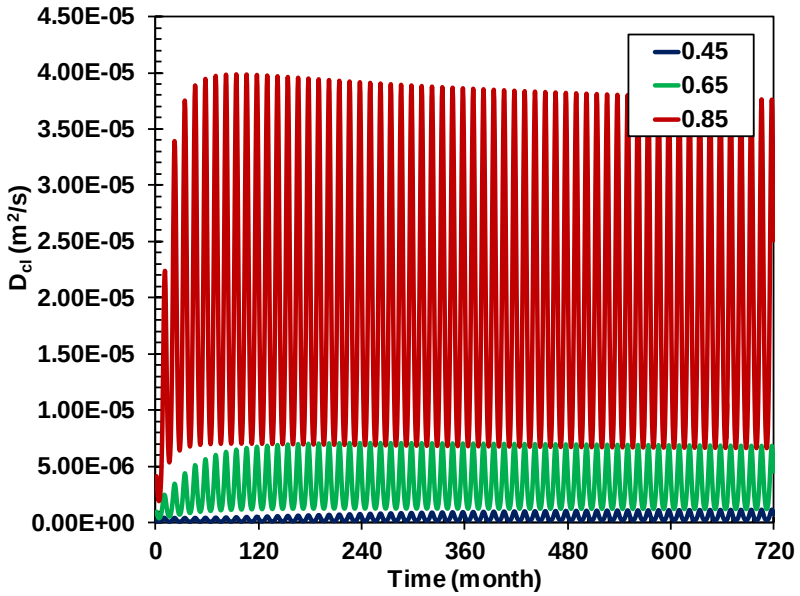

Figure 2-7. Fluctuations of D_{Cl} as a function of relative humidity

The observed trends are similar to the ones reported for the temperature effects. However, it must be noted that the variations due to temperature are much more significant than the ones due to humidity.

To study the simultaneous effect of temperature and relative humidity on chloride penetration, three exposure conditions are introduced: one average condition (Exposure II) and two extreme conditions (Exposure I and III). In Exposure II, chloride ions penetrate under the reference temperature of 291 K and a relative humidity of 0.65. For Exposure I, both mean temperature and relative humidity are decreased to 261 K and 0.45, respectively. This exposure condition is expected to majorly slow down the chloride penetration. However, the change in chloride penetration under the simultaneous increase of mean temperature and relative humidity to 321 K and 0.85, respectively, is investigated as another extreme condition. Figure 2-8 clearly captures the extent of chloride penetration in each of the three exposure scenarios after 60 years.

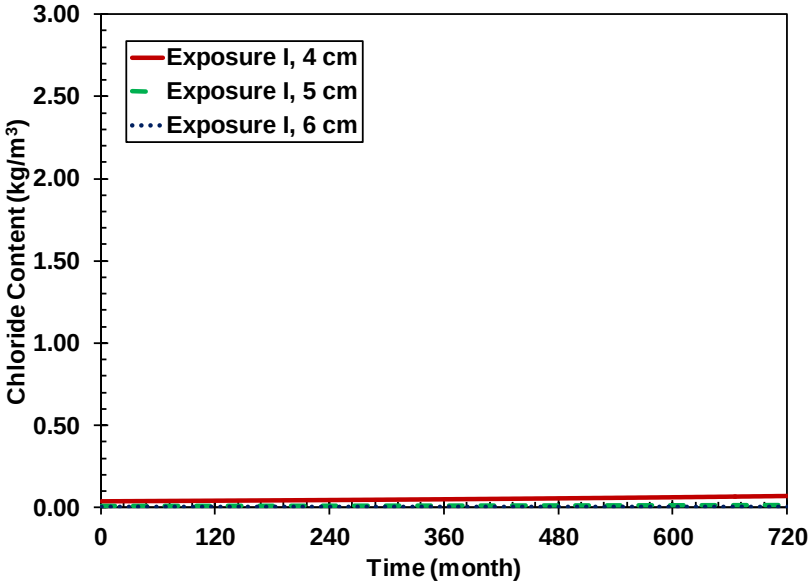
Exposure I, 4 cm
Exposure I, 5 cm
Exposure I, 6 cm
Chloride Content (kg/m³)
3.00
2.50
2.00
1.50
1.00
0.50
0.00
0
120
240
360
480
600
720
Time (month)

(a)

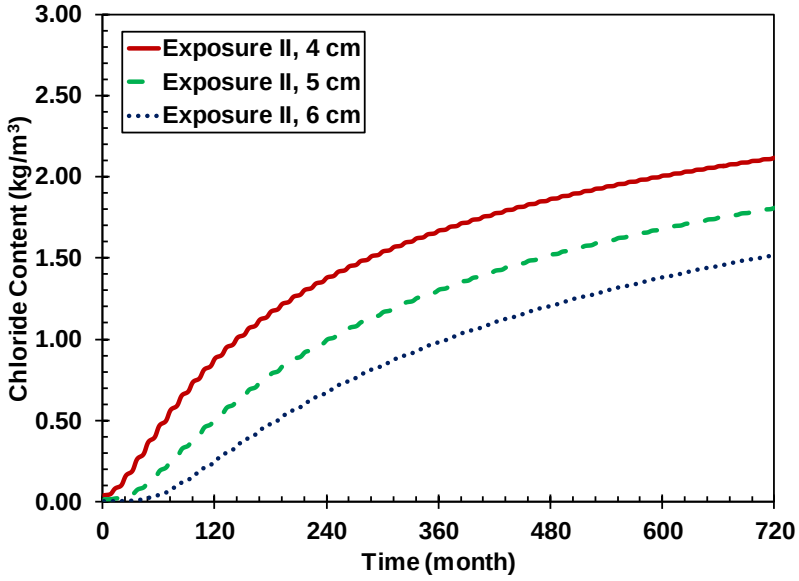
Exposure II, 4 cm
Exposure II, 5 cm
Exposure II, 6 cm
Chloride Content (kg/m³)
3.00
2.50
2.00
1.50
1.00
0.50
0.00
0
120
240
360
480
600
720
Time (month)

(b)

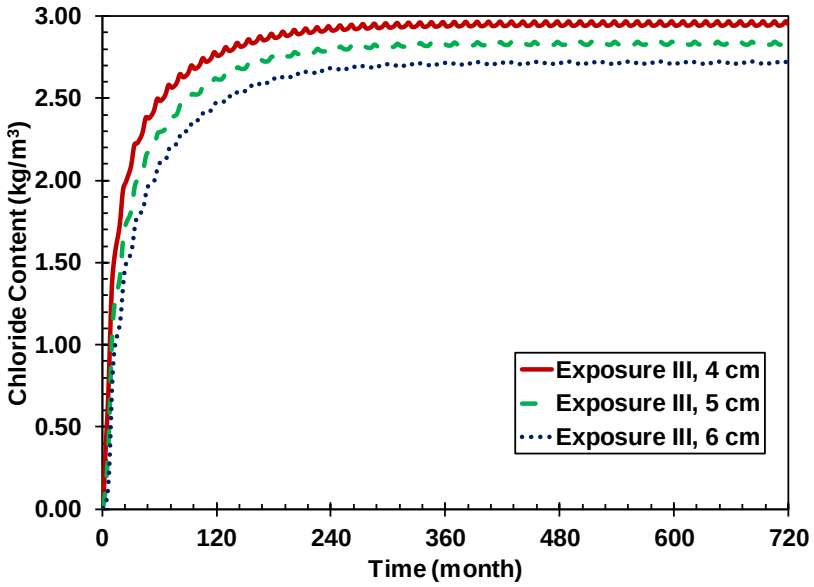

(c)

Figure 2-8. Chloride profile under Exposure I, II, and III

It is clear that as the environmental conditions become harsher (i.e., Exposure III), chloride ions penetrate into the deeper parts of the RC structure. The extent of penetration is almost negligible in Exposure I compared to Exposure III.

To quantify the impact of exposure condition, the profiles of chloride content at three different depths are plotted under Exposure I, II, and III (Figure 2-8). It can be seen in this figure that there is a major difference in the recorded chloride content among the three exposure conditions. While the chloride content is close to zero for Exposure I, it reaches 3 kg/m^3 in Exposure III. The different values of chloride concentration at the level of the rebar lead to different corrosion initiation times. The corrosion initiates when the chloride concentration at the cover depth reaches the threshold chloride concentration. The value of the threshold chloride concentration has been reported in the literature. Assuming a threshold value of 2 kg/m^3, the initiation time ranges from 2 to 50 years for Exposure II and III, respectively. The chloride content never reaches the threshold value in Exposure I.

The third external parameter investigated in the current study is surface chloride. It is clear that a high chloride content at the surface of an RC structural component creates a major gradient of concentration, which leads to a higher chloride content at deeper depths. This further increases the chloride diffusion coefficient, which is influenced by the available free chloride ions. The impact of surface chloride content on the chloride diffusion coefficient is shown in Figure 2-9 for the three surface chloride contents of 1.5, 3.5, and 5.5 kg/m^3.

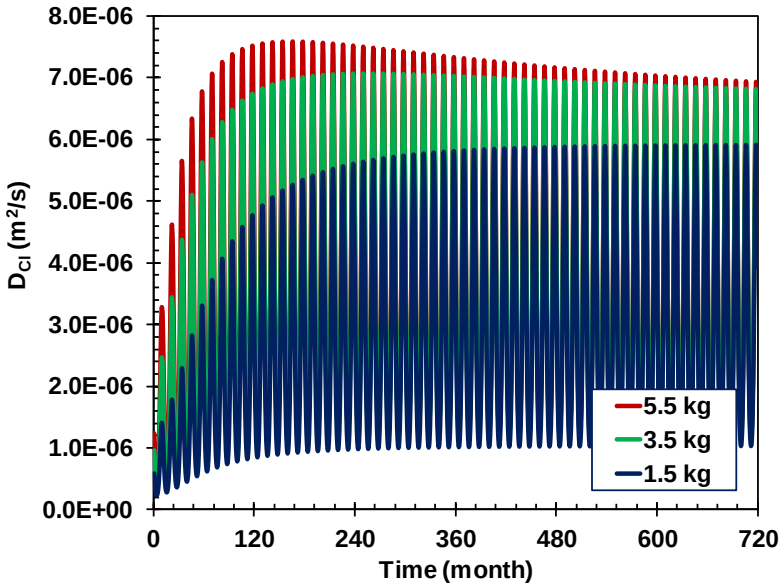

Figure 2-9. Effect of surface chloride content on the chloride diffusion coefficient over time

Figure 2-10 presents how the chloride diffusion coefficient plays a significant role in chloride penetration.

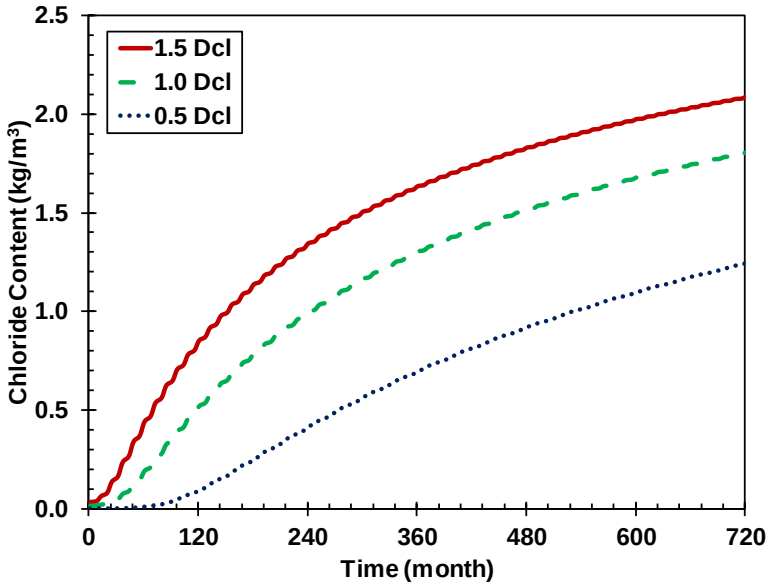

Figure 2-10. Effect of chloride diffusion coefficient on the chloride content at the rebar level

2.5. Climate Change Impact

2.5.1. Emission Scenarios

The IPCC (2014) expressed greenhouse gas (GHG) emissions through four scenarios: RCP 8.5, RCP 6.0, RCP 4.5, and RCP 2.6, in which RCP 8.5 shows high GHG emissions, RCP 4.5 and RCP 6.0 are intermediate scenarios, and RCP 2.6 reflects the stringent mitigation scenario. The trends in temperature and sea level are forecasted for these scenarios. These emission scenarios correspond to the ones in IPCC (2007), except for RCP 2.6. In IPCC (2007), the scenarios are based on the development, economic, and technological pathways. For example, A1 shows rapid economic growth and the rapid introduction of efficient technologies as well as a global population that peaks at mid-century. Based on the alternatives for technological change, A1 is divided into A1F1, which relies on fossil fuels intensively; A1T, which supplies non-fossil fuel energy resources; and A1B, which is a balance of all energy sources. A2 shows a world with high population growth but slow technological and economic development. Finally, B2 demonstrates intermediate population and economic growth. Table 2-1 summarizes the temperature variation under each of the scenarios.

Table 2-1. Predicted temperature change for the 21st century based on the fourth and fifth IPCC assessments

Scenario	Mean (°C)	Interval
Fourth assessment (IPCC 2007) 2081-2100		
RCP 2.6	1.0	0.3-1.7
RCP 4.5	1.8	1.1-2.6
RCP 6.0	2.2	1.4-3.1
RCP 8.5	3.7	2.6-4.8
Fifth assessment (IPCC 2014) 2090-2099		
B1	1.8	1.1-2.9
B2	2.4	1.4-3.8
A1B	2.8	1.7-4.4
A1T	2.4	1.4-3.8
A1F1	4.0	2.4-6.4
A2	3.4	2.0-5.4

The average temperature and humidity in Equations 2-14 and 2-15 need to be increased at each time step based on the corresponding emission. For example, if the average temperature is 20°C, it is expected to reach 23.7°C in 2100. In this study, four RCP scenarios are taken into account. Therefore, in addition to sinusoidal functions that represent the annual variation in temperature, the increasing trend of the mean of temperature is considered. There is no information available in the IPCC reports for relative humidity. Brown and Degaetano (2013) found that relative humidity has an increasing trend throughout the central region of the US but generally decreases towards the east and west coasts. Gaffen and Ross (1999) also mentioned that relative humidity has an increasing trend, especially at nights in winter and spring over most of the nation, with the most striking increase in Alaska. According to Dai (2006), the change in relative humidity is

small compared with the mean value. Dai (2006) also proposed an increasing trend for relative humidity over the central and eastern US. In order to further quantify the trend in relative humidity, three main cities of the US Midwest are selected: Chicago, Illinois; Minneapolis, Minnesota; and Des Moines, Iowa. The relative humidity in these cities can be calculated using temperature and dew point data. The data are extracted from a weather website (https://www.wunderground.com/). Figures 2-11 and 2-12 show the trends in temperature and relative humidity in these cities, respectively. It can be seen that all the three cities show a mild increasing trend for temperature, which is compatible with IPCC predictions. As for relative humidity, if the outliers are neglected, a constant or mild decreasing trend can be seen in Figure 2-12.

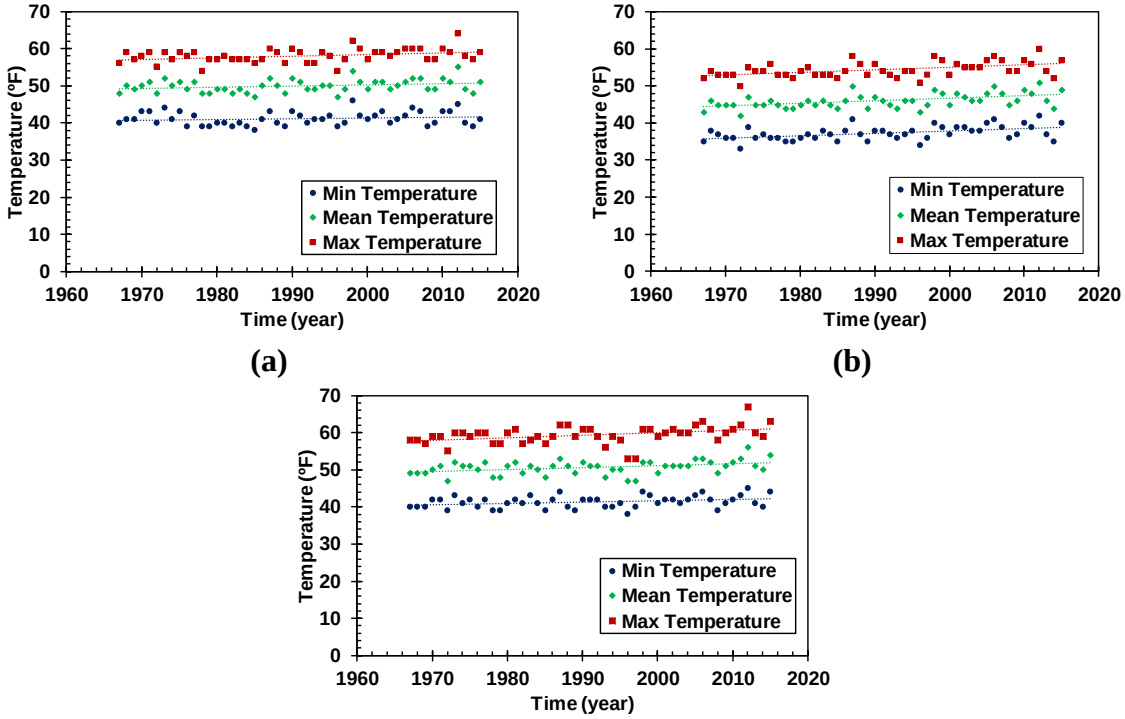

Figure 2-11. Historical temperature trends in (a) Chicago, (b) Minneapolis, and (c) Des Moines

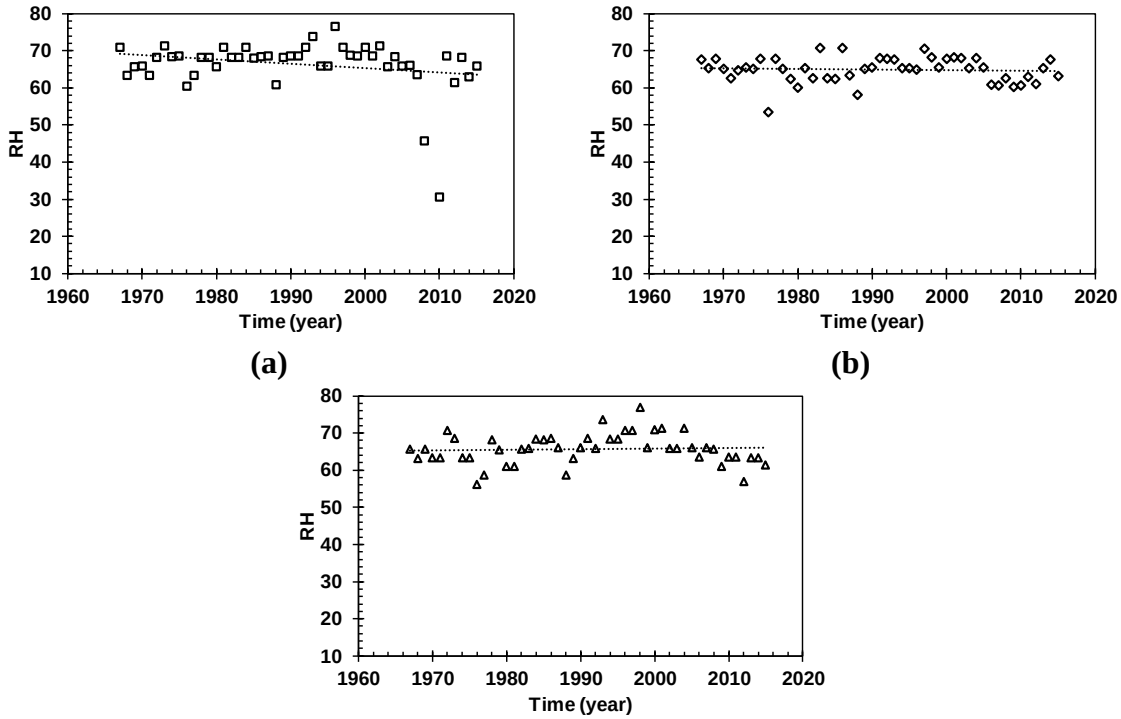

Figure 2-12. Historical trends of relative humidity in (a) Chicago, (b) Minneapolis, and (c) Des Moines

In addition to temperature and relative humidity, an estimate of the surface chloride content is necessary to model chloride penetration. Generally, there are two sources of chloride ions: deicing salts and airborne seawater salts. In the current study, it is assumed that the surface chloride is due to deicing salts used in cold seasons. Overall, the consumption of deicing salts in the US has an increasing trend (Figure 2-13a), particularly in the northern regions (Findlay and Kelly 2011).

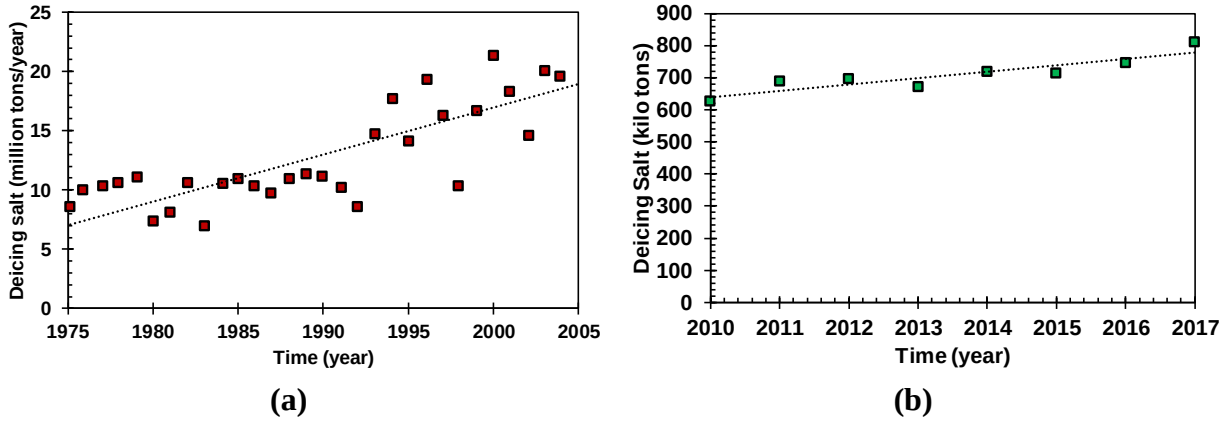

Figure 2-13. Trend of the consumption of deicing salts in the (a) northern US and (b) Iowa

This trend can be explained by extreme weather events, which are believed to be a consequence of climate change. While hotter days are expected in some regions, which can lead to the extension of droughts, the colder days in other regions lead to heavier precipitation, particularly in winter. Iowa data verifies that the use of deicing salt has increased. As shown in Figure 2-13 (b), the application of deicing salt in Iowa increases from 627 kilotons in 2010 to 810 kilotons in 2017. Knowing the fact that the number of bridges as well as lane miles of roadway are almost the same during this time interval, it can be concluded that the higher mass of deicing salt used between 2010 to 2017 may be due to extreme weather.

2.5.2. Climate Change Impact on Corrosion Initiation

To investigate the impact of climate change on corrosion initiation, temperature, relative humidity, and surface chloride are defined as time-dependent variables in FE. The variations in these parameters are defined based on Table 2-2.

Table 2-2. Variations in surface temperature, relative humidity, and surface chloride due to the impacts of climate change for three cities, Chicago, Minneapolis, and Des Moines, at the end of the 21st century

City	Temperature (°F)	Relative humidity	Surface chloride (kg/m^3)
		RCP 2.6	
Chicago	51.0-52.0	0.664-0.666	4.00-4.20
Minneapolis	48.0-49.0	0.648-0.651	4.50-4.70
Des Moines	53.0-54.0	0.657-0.659	3.50-3.68
		RCP 4.5	
Chicago	51.0-52.8	0.664-0.669	4.00-4.40
Minneapolis	48.0-49.8	0.648-0.653	4.50-4.95
Des Moines	53.0-54.8	0.657-0.662	3.50-3.85
		RCP 6.0	
Chicago	51.0-53.2	0.664-0.671	4.00-4.60
Minneapolis	48.0-50.2	0.648-0.658	4.50-5.18
Des Moines	53.0-55.2	0.657-0.664	3.50-4.03
		RCP 8.5	
Chicago	51.0-54.7	0.664-0.674	4.00-4.80
Minneapolis	48.0-51.7	0.648-0.658	4.50-5.40
Des Moines	53.0-56.7	0.657-0.667	3.50-4.20

Changes in the identified parameters influence the chloride and moisture diffusion process by varying the corresponding modification factors, $f_1(T), f_3(H), g_1(T), g_3(H)$. Figure 2-14 presents the total chloride concentration at the rebar surface over 100 years under four emission scenarios for cases where the temperature and relative humidity increase over time.

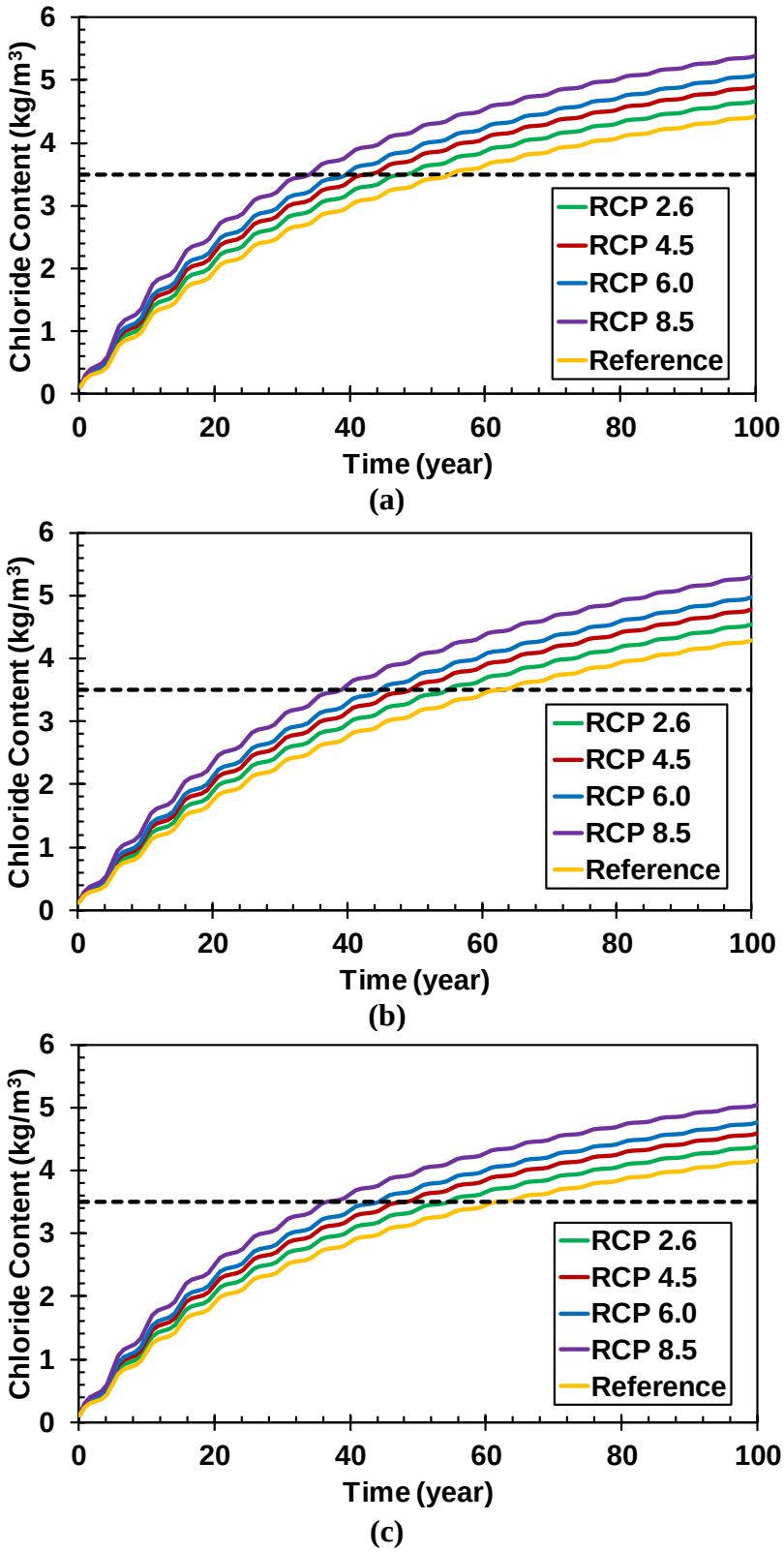

Figure 2-14. Total chloride concentration at cover depth over time in (a) Chicago, (b) Minneapolis, and (c) Des Moines

As expected, total chloride has the highest concentration under RCP 8.5 and can reach on average 22% greater than the reference case in the absence of climate change. However, the concentration of chloride content under RCP 2.6 is 6% higher than the reference case. The chloride content is similar in the three selected cities after 100 years. For example under RCP 8.5, it is equal to 5.39, 5.30, and 5.04 kg/m^3 in Chicago, Minneapolis, and Des Moines, respectively.

The profile of total chloride content can be used to evaluate the corrosion initiation time. When the chloride concentration at the rebar surface reaches the threshold chloride concentration, corrosion initiates. Val and Stewart (2003) suggested that the threshold chloride is normally distributed with a mean and coefficient of variation of 3.35 kg/m^3 and 0.375, respectively. Shafei et al. (2012) selected a threshold value equal to 3.5 kg/m^3, 1% of cement weight (350 kg/m^3), which is the proposed interval in the literature. In the current study, the threshold value is assumed to be 3.5 kg/m^3, and the corrosion initiation times are evaluated for four climate change scenarios. We calculated that the corrosion time decreases on average 13%, 22%, 29%, and 39% under RCP 2.6, RCP 4.5, RCP 6.0, and RCP 8.5, respectively. As for the total chloride content after 100 years, as the emission scenarios become more aggressive, the effect of temperature and relative humidity variation becomes more noticeable. The concentration of total chloride increases 5%, 10%, 15%, and 22% under RCP 2.6, 4.5, 6.0, and 8.5, respectively, compared to the reference case.

From the comparison of corrosion initiation time and total chloride concentration in Chicago, Minneapolis, and Des Moines, it was observed that corrosion initiates earlier in Chicago compared to the two other cities. The difference between the corrosion initiation time in Minneapolis and Des Moines is small, but it occurs earlier in Des Moines. The difference among the corrosion initiation times in these three cities can be explained by the temperature and surface chloride variations among these cities. For example, the temperature in Chicago is 1°C lower than in Des Moines while the surface chloride is 0.5 kg/m^3 greater, which leads to faster initiation of corrosion in Chicago. However, the 3°C cooler temperature in Minneapolis compared to Des Moines causes the corrosion initiation period to become longer despite the fact that surface chloride is 1 kg/m^3 greater in Minneapolis compared to Des Moines.

To incorporate the impact of climate change in bridge management systems, the chloride penetration process needs to be evaluated by incorporating the environmental parameters under different climate change scenarios. The updated chloride profile should then be employed to develop a stochastic process that can predict the future condition state of bridge components depending on site-specific exposure conditions. This can be achieved by updating the traditional transition matrices. Decision makers can then utilize the revised transition matrices to estimate the future structural condition of a bridge at any desired time interval. The details of this procedure can be found in Khatami et al. (2016). In addition to the impact of climate change on the deterioration of bridges, the severe consequences of extreme events such as flooding should be considered when decision makers plan for maintenance and repair strategies. The flowchart in Figure 2-15 highlights the key steps needed for an improved bridge management system. The cost analysis included in the flowchart includes both direct and indirect costs.

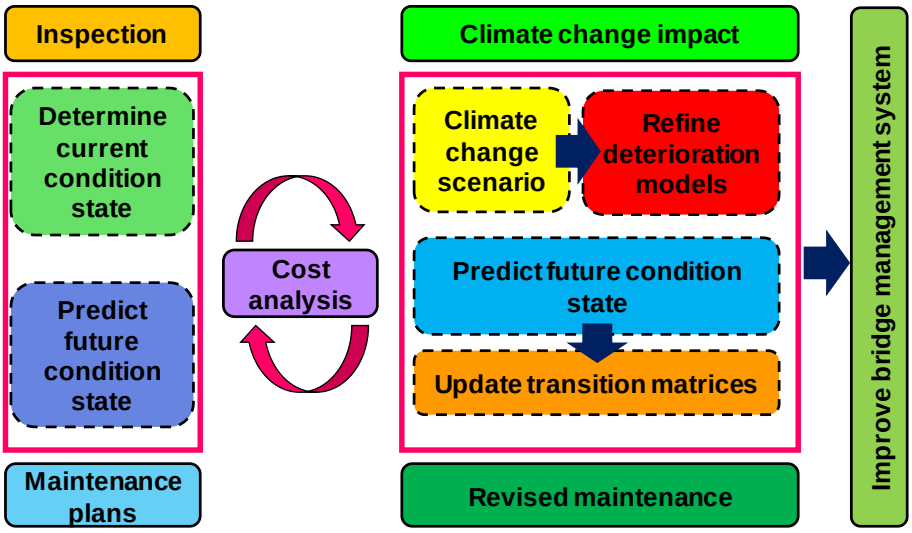

Figure 2-15. Schematic representation of improved bridge management under climate change

CHAPTER 3. PREDICTION OF DETERIORATION IN CONCRETE BRIDGES

3.1. Development of Transition Matrix

Markov transition probabilities for the deterioration of transportation network components can be determined based on the condition states obtained from visual inspections normally performed in a periodic manner. The transition probability represents the uncertain transition of the condition state during two points in time (Tsuda et al. 2006). The observed condition state of a bridge at time T_A (inspection time) is expressed by variable $s(T_A)$. The Markov transition probability, p_{ij}, provides the probability that the condition state at future time T_B becomes $s(T_B) = j$ given condition state $s(T_A) = i$ observed at time T_A (Equation 3-1).

$$P[\mathrm{s}(T_B) = \mathrm{j} | \mathrm{s}(T_A) = \mathrm{i}] = p_{ij} \tag{3-1}$$

Since it is assumed that the condition state of a deteriorating structure cannot be improved without any repair or maintenance between T_A and T_B, the transition matrix will be an upper triangular matrix. The highest level of deterioration (failure) is expressed by condition state *F*, which is recognized as an absorbing state in the Markov chain. The probability of transition out of each state is defined by a hazard function, which shows the instantaneous risk at which a component will be transitioning from its current state to a worse one. For example, the probability of remaining in condition state *i* at a subsequent time point measured from time point O_A by more than z_i is defined as follows:

$$\widetilde{F}_i\,(O_A + z_i | \varphi_i \geq O_A) = \frac{Prob(\varphi_i \geq O_A + z_i)}{Prob(\varphi_i \geq O_A)} = \frac{\widetilde{F}_i(O_A + z_i)}{\widetilde{F}_i(O_A)} \tag{3-2}$$

Using the definition of $\widetilde{F}_i(x)$ for the exponential function, Equation 3-2 becomes the following:

$$\frac{\widetilde{F}_i(y_A + z_i)}{\widetilde{F}_i(y_A)} = \frac{\exp(-\theta_i(y_A + z_i))}{\exp(-\theta_i y_A)} = \exp(-\theta_i z_i) \tag{3-3}$$

Therefore, the probability that the same condition state will be observed by a subsequent inspection time, $O_A + q$, is $\exp(-\theta_i q)$.

The Markov transition probability, p_{ij}, between any two consecutive inspections is calculated based on the conditional probabilities that can be estimated from the hazard functions. In order to make the conditional probability independent of the time period, Δ, the probability is divided by Δ to generate the hazard rate. This rate can be increasing, decreasing, or constant based on the selected hazard function and the value of its parameters. In the current study, the Markov transition probabilities are estimated using an exponential hazard model, which provides a constant hazard rate:

$$p_{ij} = \sum_{k=i}^{j} \prod_{m=i}^{k-1} \frac{\theta_m}{\theta_m - \theta_k} \prod_{m=i}^{k-1} \frac{\theta_m}{\theta_m - \theta_k} \exp(-\theta_k q) \tag{3-4}$$

where θ is referred to as the hazard rate and q is the inspection interval. For the special cases of remaining in state i, p_{ii}, degrading only one state from state i to $i+1$, p_{ii+1}, and degrading from state i to state F, p_{iF}, Equation 3-4 can be simplified to the following:

$$p_{ii} = \exp(-\theta_i q) \tag{3-5}$$

$$p_{ii+1} = \frac{\theta_i}{\theta_i - \theta_{i+1}}\{-\exp(-\theta_i q) + \exp(-\theta_{i+1} q)\} \tag{3-6}$$

$$p_{iF} = 1 - \sum_{j=i}^{F-1} p_{ij} \ \ (i = 1, \dots, F-1) \tag{3-7}$$

3.2. Prediction of Condition States

Based on the inspection results, the state of deterioration and extent of damage to deteriorating structures can be determined. Without appropriate maintenance actions, the condition state continuously degrades, and the consequences of the deterioration processes become apparent from the spalls, splits, and cracks (Bu et al. 2014, Ranjith et al. 2013) or from the signs of corrosion, such as change of color and accumulation of aggressive agents (Saydam et al. 2013, Shafei et al. 2012). In the current study, five condition states are introduced based on the concentration of chloride ions at the rebar surface. The exposure to chloride ions can originate either from airborne sea salts or deicing salts used in wintertime. By utilizing a detailed transient analysis that can capture the uncertainties inherent in material properties and exposure conditions (Shafei et al. 2013), the profile of chloride ions is calculated for a comprehensive set of surface chloride contents, concrete durability levels, and rebar cover depths, as explained in Chapter 2.

Based on the predicted chloride profile, the state of deterioration can be identified. Since it has been shown that there is a direct correlation between the condition state and chloride content, the values summarized in Table 3-1 are utilized to quantify the state of deterioration.

Table 3-1. Correlation between the predicted chloride content and state of deterioration

Condition State	Description
1	$0.0 \leq [Cl] \leq 0.5$ kg/m^3 (new or near new)
2	$0.5 \leq [Cl] \leq 1.0$ kg/m^3
3	$1.0 \leq [Cl] \leq 2.0$ kg/m^3
4	$2.0 \leq [Cl] \leq 5.0$ kg/m^3
5	$5.0 \leq [Cl]$ kg/m^3 (susceptible to failure)

In this table, Condition State 1 represents an excellent condition, in which the structure is either intact or has negligible deterioration. As deterioration advances, the condition state increases until it reaches Condition State 5, in which the serviceability and performance of the structure comes into question because of the propagated damage.

Since the hazard function can be expressed in terms of factors that reflect the exposure conditions and structural characteristics, vector x with two variables, x_1 and x_2, is introduced to predict the duration of time in which the k-th structure maintains the i-th condition state based on the surface chloride concentration and rebar cover depth:

$$\theta_i^k = \beta_{i,1} + \beta_{i,2}x_1^k + \beta_{i,3}x_2^k \tag{3-8}$$

where β is a vector that relates the hazard rate to the parameters affecting the deterioration process (i.e., surface chloride concentration and rebar cover depth). The estimated β parameters for four condition states are shown in Table 3-2. Since Condition State 5 is an absorbing state, there is no need to calculate the β parameters for it because the failure probabilities can be obtained directly from Equation 3-7.

Table 3-2. Estimated parameters for the exponential hazard model

State	$\boldsymbol{\beta_{i,1}}$	$\boldsymbol{\beta_{i,2}}$	$\boldsymbol{\beta_{i,3}}$
1	-0.0164	-0.3208	0.9075
2	0.5155	-0.3809	0.1553
3	0.4772	0.2457	-0.6126
4	0.1280	0.4721	-0.5243

From the obtained β parameters, the Markov transition probability matrix is formed following the procedure explained in the previous section. To investigate the effects of inspection intervals, one-year and three-year inspection intervals, in addition to a two-year inspection interval, which is recommended for highway bridges in the United States, are considered to evaluate the sensitivity of the results to the frequency of field data collection. Table 3-3 summarizes the transition probability matrices for the three inspection plans. It can be observed that the probability of remaining in Condition State 1 decreases as the inspection interval increases.

Table 3-3. Transition probabilities matrices for 1-, 2-, and 3-year inspection intervals

Inspection Interval	State	1	2	3	4	5
1 year	**1**	0.7140	0.2471	0.0354	0.0033	0.0002
	2	0	0.7538	0.2141	0.0295	0.0026
	3	0	0	0.7613	0.2102	0.0285
	4	0	0	0	0.7804	0.2196
	5	0	0	0	0	1.0000
2 years	**1**	0.5099	0.3628	0.1051	0.0196	0.0027
	2	0	0.5682	0.3244	0.0902	0.0171
	3	0	0	0.5796	0.3241	0.0963
	4	0	0	0	0.6090	0.3910
	5	0	0	0	0	1.0000
3 years	**1**	0.3641	0.3994	0.1757	0.0497	0.0111
	2	0	0.4283	0.3686	0.1554	0.0477
	3	0	0	0.4413	0.3747	0.1840
	4	0	0	0	0.4753	0.5247
	5	0	0	0	0	1.0000

3.3. Cost Analysis

The operational cost is an important concern for the functionality of a transportation network. As the network becomes more complex and its expected life-cycle increases, the maintenance costs gradually add up and may reach a level that greatly influences the decisions made regarding the future of deteriorating components. To address this concern, cost-effective preventive maintenance policies can be employed to reduce the total cost and number of structural failures while extending the service lives of structures (Lu et al. 2007). According to the FHWA, the average cost of replacing corroded highway bridges during the period from 1992 to 2002 was $3.8 billion (Lee 2012). Fernando et al. (2012) studied the most sustainable intervention strategies for bridges and concluded that intervention costs, travel costs, and vehicle operation costs have the most significant impacts on such strategies.

The life-cycle cost (LCC) of a structure consists of the initial construction and operational costs. LCC analysis can help allocate appropriate resources for the design, construction, and operation of the structure. In the current study, the main focus is to minimize the operational cost of transportation network components that may lose their structural capacity due to the corrosion process. To obtain the total LCC of deteriorating structures, the following equation is utilized:

$$\text{LCC} = C_c + [C_{IN} + C_M + C_M^u] \tag{3-9}$$

where C_c is the initial construction cost, C_{IN} is the inspection cost, C_M is the maintenance cost, and C_M^u is the indirect cost due to maintenance activities (e.g., temporary closure of facilities and travel delays). The future maintenance expenditure is calculated based on the base year price

using a discount factor, α, that takes into account the time value of the money. This factor is defined in terms of interest rate i as follows:

$$\alpha = (1 + i)^{-1} \tag{3-10}$$

In practice, the discount rate is typically in the range of 2% to 8% depending on the economic situation and prospect. A high discount rate is suitable for a short service time, while a low discount rate favors a longer service time. To illustrate the probabilistic framework developed in the current study, the operational cost of a medium-span bridge located in Los Angeles, California, is evaluated (Alipour et al. 2011 and 2013). To identify the most appropriate maintenance actions, both cost-based and condition-based actions are examined. This analysis includes four different maintenance actions and three different inspection intervals to evaluate a range of actions currently taken in practice. The first set of actions is cost-based, which means that the budget is limited and that reaching a specific level of expenditure may dictate changes in the maintenance plans. Contrary to the cost-based strategies, the proposed condition-based strategies are assumed not to be affected by budget limitations to maintain certain condition states. Table 3-4 provides more detailed information about the four courses of action, which are further evaluated in the next section.

Table 3-4. Cost-based and condition-based maintenance actions

Action	Description
1	Step 1: Current state improves to Condition State 1 Step 2: Current state improves to Condition State 2 if $(C_{IN} + C_M + C_M^u) > C_c$
2	Step 1: Current state improves to Condition State 1
3	Step 1: No action until the bridge condition reaches Condition States 4 and 5 Step 2: Current state improves to Condition State 1
4	Step 1: Current state improves to the previous condition state

The four actions considered along with the three inspection intervals form a set of 12 scenarios for improving the performance and safety of aging components. It is necessary to mention that the inspection cost is constant for all of the condition states; however, the maintenance cost depends on the current state and changes based on the extent of improvement recommended by decision-making authorities.

3.4. Assessment of Human Judgment Factor

It has been found that when a group of experts is asked to evaluate the condition state of a specific bridge based on identical inspection data, their opinions about the state of deterioration can be completely different. Such variation in expert opinions is a result of a wide range of parameters, including experience, training, and even personal characteristics. Although the deviation of the estimated condition state from the actual state of a structure can be justified, its consequences for maintenance planning and budget allocation cannot be neglected. To address this issue, it is necessary to capture the effects of expert judgment discretion and the uncertainties

associated with it using a probabilistic approach. The thinking process of experts in arriving at a judgment about the condition state of a deteriorating structure can be explained by Brunswikian theory. Adelman et al. (2003) used Brunswikian theory to study how hierarchical teams adapt to increasing levels of time pressure. They simulated an air defense task with three team members (a leader and two subordinates) and evaluated their judgments on an aircraft's hostility level. Kirlik (2010) used the same theory to model clinical judgment in a representative experimental condition.

The lens model presented by Brunswik (1952) represents a situation where an individual or expert makes a decision about the true state of a distal variable based on the available information. The extended lens model, named the multi-level lens model, was presented by Brehmer and Hagafors (1986). The multi-level model involves an intermediate process, in which subordinate staff make recommendations based on existing information and pass those recommendations to the expert to make the final decision. Gigerenzer et al. (1991) proposed probabilistic mental models for cognitive processes in judgment. These models characterize the thinking process with respect to various confidence levels. In order to consider the expert judgment factor in predicting the future condition of deteriorating structures, probabilistic mental models have been utilized in the current study. For this purpose, three groups of experts are asked to identify the condition state of a set of deteriorated bridges, and then a confidence level is assigned to the estimated numbers. To quantify the confidence level, a confidence scale consisting of seven levels (i.e., I through VII) is provided. Starting from I and ending at VII, this confidence scale represents 0%, 1% to 20%, 21% to 40%, 41% to 60%, 61% to 80%, 81% to 99%, and 100% confidence levels, respectively. For the purpose of this LCC analysis, the mean values of the confidence levels are used to update the transition matrix at each time interval.

To start the analysis, it is assumed that the structure is in Condition State 1 (i.e., new or near-new condition). The condition state is then updated at each time step based on both the transition matrix and human judgment factor. This is one of the unique contributions of the current study to further improve the accuracy of life-cycle performance predictions of deteriorating structures. To better understand the contribution of human judgment, three categories of human judgment are investigated and the obtained results are compared with the ones that neglect this factor. The first and third categories consist of "optimistic" and "pessimistic" experts who constantly exaggerate the actual condition of the structure to a better and worse condition, respectively. The second category includes "realistic" experts. The realistic experts are expected to make an unbiased judgment, although their level of confidence may vary because of their level of experience and training. Table 3-5 summarizes the confidence levels assigned to each of the three categories of experts. It should be noted that if realistic experts estimate each condition state with the highest confidence level (i.e., VII), the predicted condition state will be the same as the one predicted without considering the human judgment factor.

Table 3-5. Confidence level matrices for three categories of experts

Expert categories	Condition State														
	Optimistic					Realistic					Pessimistic				
	1	2	3	4	5	1	2	3	4	5	1	2	3	4	5
Confidence level	VII					VII					II	VII			
	VII	II					VII					II	VII		
		VII	II					VII					II	VII	
			VII	II					VII					II	VII
				VII	II					VII					VII

Considering the potential consequences of the human judgment factor, the LCCs of the deteriorating structures under investigation are calculated for all 12 scenarios introduced in the previous section. Figure 3-1 illustrates the results of the cost analyses for the three categories of experts.

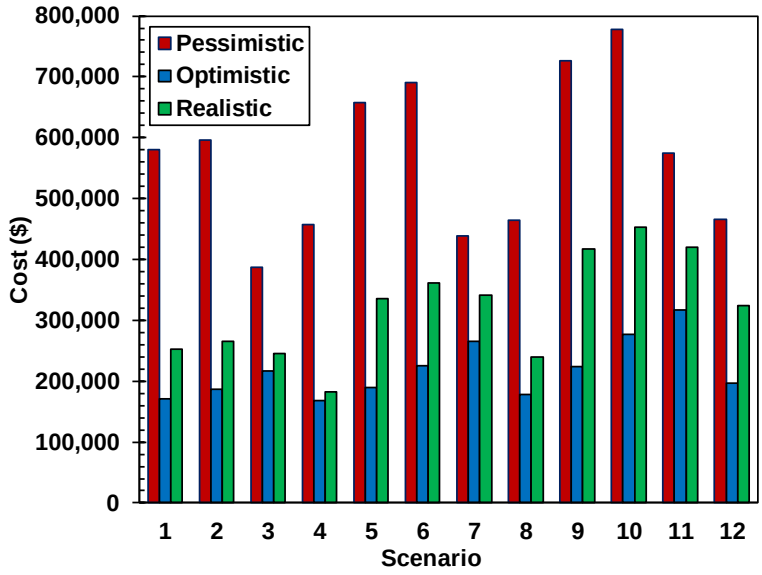

Figure 3-1. LCC analyses for different inspection intervals and maintenance actions, including the human judgment factor

It is evident that the operational costs predicted by the optimistic and pessimistic experts are always lower and higher, respectively, than those estimated by the realistic experts. Nevertheless, the estimates obtained from the category of optimistic experts tend to be closer to the ones provided by the category of realistic experts. Among all of the proposed scenarios, the one that aims at improving the existing condition state to Condition State 1 in every year is found to be the most optimized strategy for both the optimistic and realistic categories. This, however, is not the case for the pessimistic category, which favors an improvement to Condition State 1 every three years. It should be noted that the optimized cost predicted by the pessimistic experts is almost as twice as high as the costs obtained from the other two categories of experts.

3.5. Confidence Level and Weight

In addition to the categories discussed earlier, there has always been a concern about the level of confidence of the inspectors. Although the realistic experts tend to deliver unbiased predictions, their confidence level may affect maintenance plans and estimated costs. To measure this factor, the category of realistic experts is divided into three subcategories, each with a certain level of confidence. This is reflected in the confidence level matrices listed in Table 3-6.

Table 3-6. Confidence level matrices for three subcategories of realistic experts

Expert categories	Condition State														
	Realistic														
	1	2	3	4	5	1	2	3	4	5	1	2	3	4	5
Confidence level	VII	II				VI	III				V	IV			
	II	VII	II			III	VI	III			IV	V	IV		
		II	VII	II			III	VI	III			IV	V	IV	
			II	VII	II			III	VI	III			IV	V	IV
				II	VII				III	VI				IV	V

The LCC calculated for each of these three subcategories is shown in Figure 3-2. In all of the scenarios under consideration, as the confidence level decreases from VII to V, the operational cost increases, highlighting the importance of proper training and clear inspection criteria.

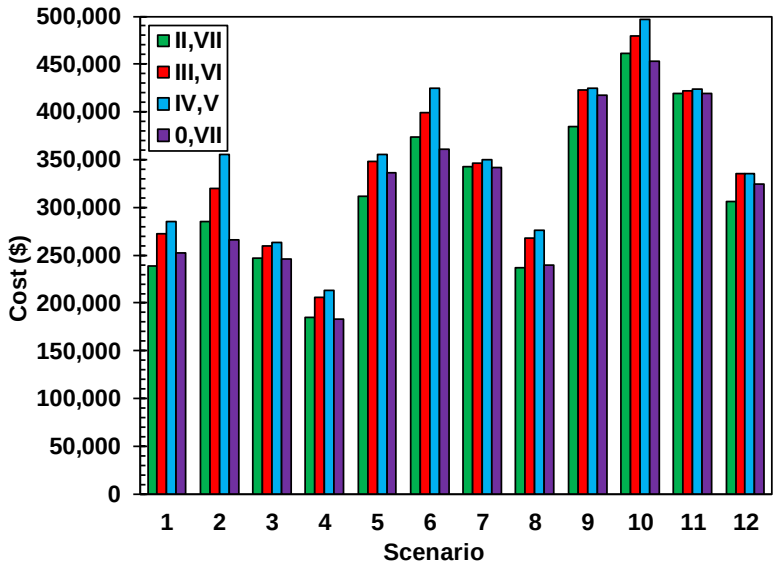

Figure 3-2. LCC analyses for the category of realistic experts with different confidence levels

If a group of *e* experts makes independent judgments using the same set of information, the condition state of the deteriorating structure can be estimated by a weighted average:

$$\boldsymbol{P} = \sum_{i=1}^{e} w_i \boldsymbol{P}_i \quad (3\text{-}11)$$

where P_i is the condition state vector based on the *i*-th expert judgment and the w_i is the weight reflecting the accuracy of the *i*-th expert in making a judgment. The weight associated with an expert can be calculated from the following:

$$w_i = r_{ai}^m / \sum_{i=1}^{n} r_{ai}^m \ (m \geq 0) \quad (3\text{-}12)$$

where r_{ai}^m is the achievement factor of the *i*-th expert determined from the previous cases and *m* is the degree of importance (Rao et al. 2004). In this study, three experts from each of the three categories are asked to evaluate the condition state. All of the experts have equal capability in terms of qualification and have access to the same information. The achievement factor of each expert is determined by a linear regression model. Because of the uncertainty inherent in the achievement factor, a set of cases is considered in the current study for weighting the expert judgment. In these cases, an achievement factor of 0.95, 0.85, and/or 0.75 is randomly assigned to the realistic, pessimistic, and optimistic experts, respectively. Based on the outcome of the performed analyses, Figure 3-3 summarizes the percentage of changes in the estimated LCC when a higher weight factor is considered for either the pessimistic or optimistic category in comparison to the realistic one.

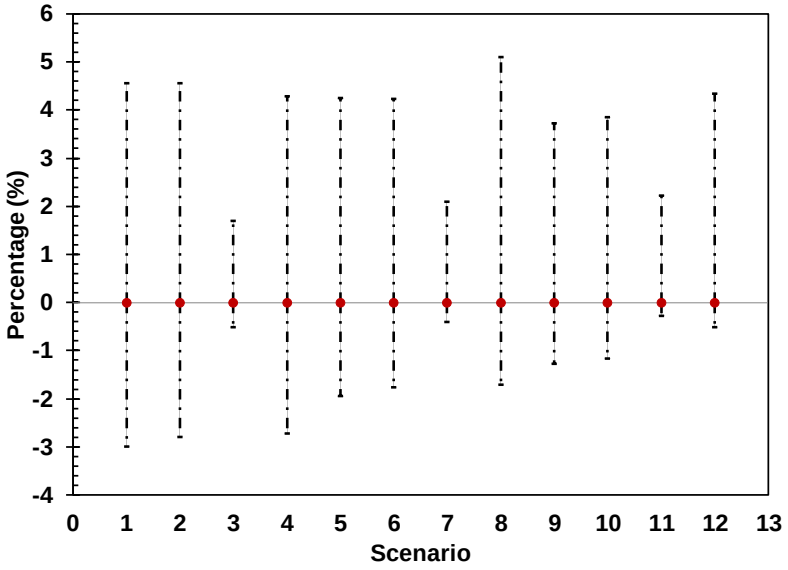

Figure 3-3. Percentage of changes in the estimated operational cost considering a weight factor for the three categories of experts

This result clearly highlights the level of contribution of the human judgment factor to the decision-making algorithms that take into account the condition states of aging network components.

3.6. Transition Matrix due to Extreme Events

Bridge management systems utilize a stochastic Markovian methodology to identify a bridge's condition state during the expected service life. The current systems are, however, mainly focused on deterioration processes and do not take into account the degradation of the condition state due to sudden extreme events, such as earthquakes. The cascading effects of aging mechanisms and earthquake events on the capacity loss of bridges have been confirmed and quantified through a number of research efforts. Among them, Choe et al. (2009) and Simon et al. (2010) considered the effects of capacity reduction on the seismic performance of corroding bridges. The studies, however, lack an investigation of the nonlinear time-dependent parameters that influence the corrosion process. Alipour et al. (2011 and 2013) developed a computational methodology to study how corrosion adversely affects the long-term performance of reinforced concrete bridges. The study revealed that the lateral load resistance of a bridge gradually drops after the corrosion initiation time, primarily due to cracks in the concrete and a loss of mass in the steel rebars. The study also explored the degradation of the performance of bridges subjected to three sets of ground motions while the bridges were exposed to the attack of chloride ions at the same time.

Based on the wealth of knowledge available in the literature, the current study introduces one of the first systematic efforts to incorporate the probability of the occurrence and potential consequences of natural hazards into bridge management systems. For this purpose, the Markovian transition matrices discussed in previous sections are modified by integrating hazard characteristics. Each natural hazard may cause either structural failure or degradation depending on the intensity of the hazard and the condition state of the bridge elements. Therefore, a set of transition matrices is generated in the current study to capture the effects of earthquakes on deteriorating bridges. The proposed methodology is designed to be conveniently added to existing bridge management systems to improve the accuracy of predictions for single and even multiple hazards.

To calculate the corresponding transition probabilities, fragility curves are utilized to statistically evaluate the expected response of bridges under region-specific seismic hazards. Seismic fragility is a relationship between the ground motion intensity that excites a structure and the probability of damage to the structure exceeding specific limit states. Fragility curves can be developed either empirically using data collected from past earthquakes or analytically using representative bridge models and ground motion records. In the fragility models, the extent of damage is typically defined in terms of discrete categories, such as light, moderate, and severe. Therefore, fragility curves are generated by estimating the probability of exceeding predefined damage states under a range of possible ground motion intensity measures, such as peak ground acceleration (PGA). A two-parameter, i.e. median μ_j and log-standard deviation σ_j, lognormal distribution is used in the current study to express the fragility curves (Shinozuka et al. 2000). For the *j*-th damage state, the fragility curve is developed following the formula below:

$$F_j\left(PGA_i \middle| \sigma_j, \mu_j\right) = \Phi\left[\frac{\ln\left(PGA_i/\mu_j\right)}{\sigma_j}\right] \tag{3-13}$$

where F_j reveals the probability of exceeding the damage state of j and $\Phi[.]$ indicates the standard normal distribution function. Figure 3-4 shows the fragility curves obtained for one of the representative two-span bridges, which has a medium span length and column height of 10 m.

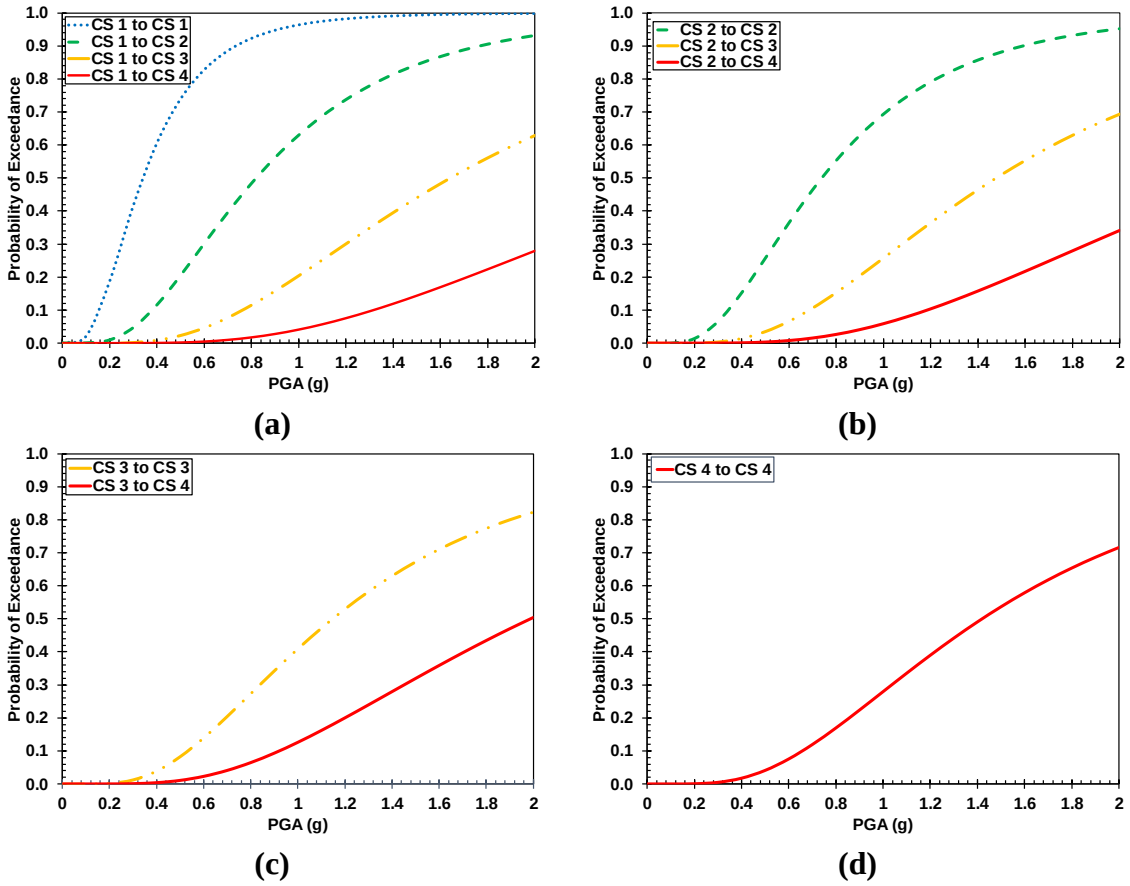

Figure 3-4. Developed fragility curves for the representative two-span bridge in each of the four condition states: (a) Condition State 1, (b) Condition State 2, (c) Condition State 3, and (d) Condition State 4

It can be seen in this figure that depending on the current condition state, the bridge may stay in the same condition or degrade to a worse one based on the intensity of the ground motion. It must be noted that the fragility curves are not generated for the last condition state because it is an absorbing one. The absorbing state is a state that, once entered, cannot be left, e.g. failure of the bridge.

As mentioned before, seismic events are considered in the current study to be extreme events. A set of three hazard risks, including low, medium, and high, are investigated to understand the effects of site-specific earthquakes with different intensities (a range of PGA values) on the life-cycle performance and cost of bridges. It should be noted that, contrary to deterioration processes, as the level of expected seismic hazard increases, its corresponding probability of occurrence decreases. Therefore, for the proper incorporation of seismic hazard in the Markovian

matrix, it is necessary to know the probability of occurrence of various ground motion intensities in addition to their effects on the bridge elements. To achieve this goal, site-specific hazard curves are paired with the fragility curves. Seismic hazard analysis helps to quantify the probability of exceeding various ground motion intensities at a site, given all possible earthquake scenarios. Figure 3-5 shows three seismic hazard curves obtained from the US Geological Survey (USGS) for bridges located in southern California.

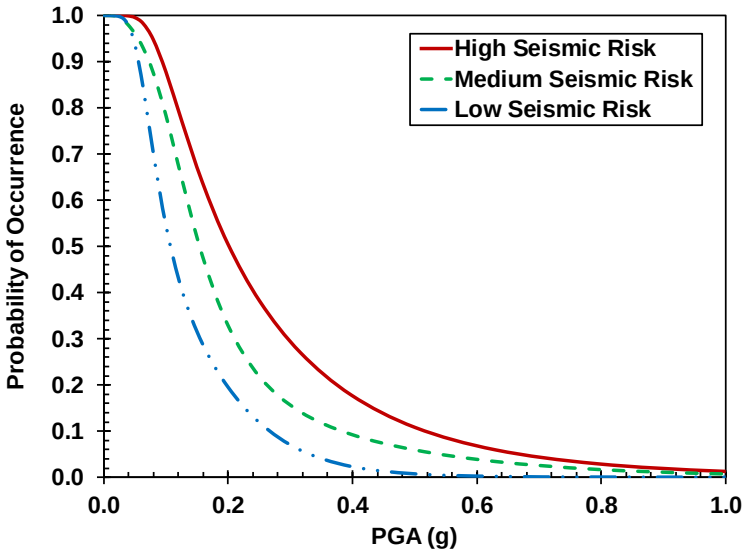

Figure 3-5. Hazard curves for three different seismic hazard risks obtained from USGS

For example, in a region with a medium seismic risk, the probability of occurrence of an earthquake with a PGA of 0.5 g equals 0.06, which means that a bridge under the impact of such an earthquake will transition from the current condition state to other deterioration states with a probability of 0.06 multiplied by the corresponding earthquake transition matrix (Table 3-7).

Table 3-7. Transition probabilities matrix due to earthquake events

State	1	2	3	4	Beyond
		PGA=0.50g			
1	0.26	0.53	0.18	0.02	0.00
2	0.00	0.67	0.28	0.04	0.00
3	0.00	0.00	0.80	0.18	0.03
4	0.00	0.00	0.00	0.80	0.20
Beyond	0.00	0.00	0.00	0.00	1.00
		PGA=0.75g			
1	0.11	0.49	0.32	0.07	0.01
2	0.00	0.49	0.39	0.10	0.02
3	0.00	0.00	0.67	0.26	0.07
4	0.00	0.00	0.00	0.70	0.30
Beyond	0.00	0.00	0.00	0.00	1.00
		PGA=1.00g			
1	0.04	0.33	0.42	0.16	0.04
2	0.00	0.29	0.45	0.20	0.06
3	0.00	0.00	0.50	0.34	0.15
4	0.00	0.00	0.00	0.56	0.44
Beyond	0.00	0.00	0.00	0.00	1.00

Based on the available data, Markovian transition matrices are calculated for all of the possible earthquake intensities in the region. The results for three specific PGA values, 0.5 g, 0.75 g, and 1.0 g, are summarized in Table 3-7. It is clear that as an earthquake becomes more severe, the probability of experiencing structural degradation and damage increases. This trend is more obvious for Condition States 3 and 4.

Based on the calculated Markovian transition matrices for aging mechanism and seismic hazard, the future condition of bridges can be estimated. The evolution of a Markov chain is expressed through the Chapman-Kolmogorov equation. Therefore, the state of the Markov chain at time n, $\mu^{(n)} = P(x_n = i)$ is estimated as follows:

$$\mu^{(n)} = \mu^{(0)} P^n \tag{3-14}$$

where P^n denotes the nth power of matrix P. Hence, in order to calculate the state of the Markov chain at time n, all we need is the initial distribution $\mu^{(0)}$ and the transition matrix P. Figure 3-6 shows the average condition of a bridge in the next 10 years under only the aging mechanism as well as under the simultaneous effects of the aging mechanism and earthquakes.

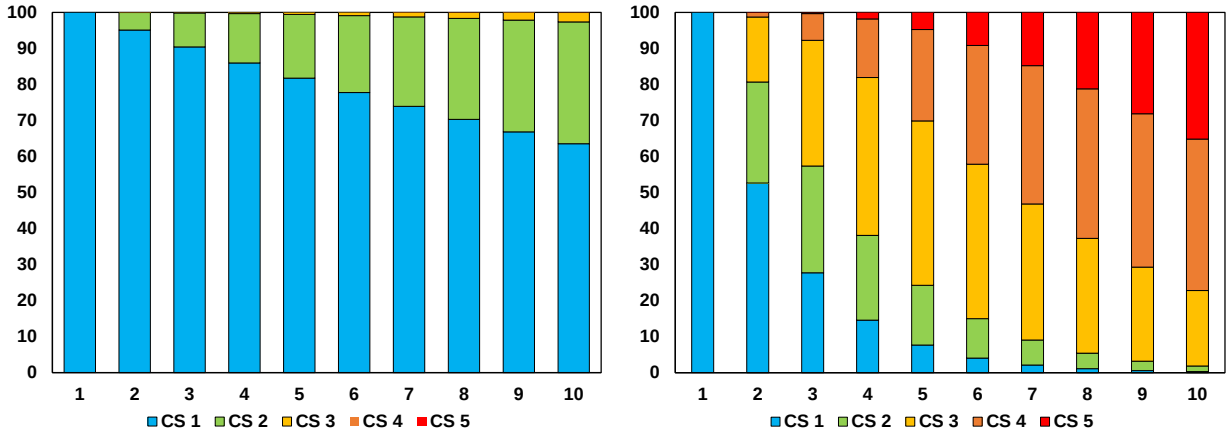

Figure 3-6 Prediction of future condition state of a bridge in next 10 years assuming that the bridge is in Condition State 1 initially under (a) only the aging mechanism and (b) the simultaneous effects of the aging mechanism and seismic hazard

It can be observed that considering only the aging mechanism, the future condition of the bridge is underestimated, and therefore planning for maintenance/repair actions will be inaccurate and, consequently, the required budget for improvement actions will be imprecise. The life-cycle cost of a bridge is calculated for the case where only the aging mechanism is considered and the case where both the aging mechanism and seismic hazard are taken into account. The results of the LCC analysis reveal that the estimated cost considering both gradual and sudden degradation is approximately 45% higher than the cost due to gradual aging only.

CHAPTER 4. SUMMARY

To predict the future condition of RC structures and plan for optimized repair and maintenance actions, it is critical to evaluate the extent of degradation over time. Since chloride penetration is the main source of degradation for RC structures, the current study developed a comprehensive finite element model to capture the effects of the most important external and internal parameters related to chloride content at different depths of RC structures. Moreover, the corrosion process in the bridge elements was modeled comprehensively using the CA framework. It was revealed that both the FE and CA methods are capable of generating chloride profiles in reasonable agreement with experimental results. The impacts of uncertainty and variation on the parameters involved in the deterioration process were fully investigated. It was realized that temperature is a significant parameter in the reinforcement corrosion process.

To study the effects of variations in temperature, relative humidity, and surface chloride over the next 100 years, climate change scenarios were defined and implemented in the developed FE framework. Environmental data for three cities in the US Midwest region, Chicago, Des Moines, and Minneapolis, were gathered in order to incorporate their effects into the chloride penetration process. Incorporating the parameters of climate change scenarios into the developed finite element models, chloride concentrations were simulated at the level of the rebars in RC structures. It was observed that corrosion initiation time decreases on average 13%, 22%, 29%, and 39% under RCP 2.6, RCP 4.5, RCP 6.0, and RCP 8.5, respectively.

In addition to the aging mechanism, which results in a gradual degradation in condition, the occurrence of extreme events such as flooding, earthquakes, and hurricanes can cause an abrupt reduction in the functionality of bridges. In this study, a comprehensive risk-based framework was developed to evaluate the future condition state of bridges by taking into consideration the simultaneous effects of gradual deterioration (e.g., aging) and extreme events (e.g., earthquakes). This model is designed to be directly implemented into existing bridge management systems to determine the damage condition of bridges with greater accuracy and consequently identify the most appropriate maintenance strategies. The condition states of bridges are estimated using a Markovian transition matrix. The Markovian matrix consists of two separate matrices capturing the effects of both aging and earthquake events. The entries of the aging matrix are calculated according to a hazard function, while the earthquake matrix is estimated based on fragility and hazard curves. The difference between considering and not considering an extreme event in the management of bridges was shown through life-cycle cost analyses, and it was concluded that the incorporation of natural hazards into bridge management systems plays an important role in determining the required maintenance budget, providing the best maintenance strategies, and planning for emergency response actions. This is completely in line with the objectives of MAP-21 and directly helps transportation agencies minimize both direct and indirect costs.

In order to generate the Markovian matrix representing the aging mechanism, determining the most recent state of degradation of a bridge is required. Recognizing the fact that the identification of the actual condition state plays an important role in the management of aging components, a comprehensive stochastic approach was proposed in the current study to understand the human judgment factor and quantify its effects on the total operational costs. This

was achieved through a systematic investigation of stochastic deterioration processes, hazard functions, and probabilistic mental models. By considering a range of practical inspection intervals and maintenance actions, the contribution of expert opinion to life-cycle performance and cost analyses was measured using three categories reflecting various cases in which the predicted condition state is different from the actual one. It is expected that the outcome of this study can be directly implemented into the current decision-making algorithms to improve the management of transportation network components by taking into account the errors and uncertainties originating from human judgment.

REFERENCES

Ababneh, A., F. Benboudjema, and Y. Xi. 2003. Chloride Penetration in Non-Saturated Concrete. *Journal of Materials in Civil Engineering*, Vol. 15, No. 2, pp. 183–191.

Adelman, L., S. L. Miller, D. Henderson, and M. Schoelles. 2003. Using Brunswikian Theory and a Longitudinal Design to Study How Hierarchical Team Adapt to Increasing Levels of Time Pressure. *Acta Psychologica*, Vol. 112, No. 2, pp. 181–206.

Agrawal, A. K., A. Kawaguchi, and Z. Chen. 2010. Deterioration Rates of Typical Bridge Elements in New York. *Journal of Bridge Engineering*, Vol. 15, No 4, pp. 419–429.

Alipour, A., B. Shafei, and M. Shinozuka. 2011. Performance Evaluation of Deteriorating Highway Bridges Located in High Seismic Areas. *Journal of Bridge Engineering*, Vol. 16, No. 5, pp. 597–611.

Alipour, A., B. Shafei, and M. Shinozuka. 2013. Capacity Loss Evaluation of Reinforced Concrete Bridges Located in Extreme Chloride-Laden Environments. *Structure and Infrastructure Engineering*, Vol. 9, No. 1, pp. 8–27.

Bamforth, P. B. 1999. The Derivation of Input Data for Modelling Chloride Ingress from Eight-Year UK Coastal Exposure Trials. *Magazine of Concrete Research*, Vol. 51, No. 2, pp. 87–96.

Bastidas-Arteaga E. and M. G. Stewart. 2015. Economic Assessment of Climate Adaptation Strategies for Existing Reinforced Concrete Structures Subjected to Chloride-Induced Corrosion. *Structure and Infrastructure Engineering*, Vol. 12, No. 4, pp. 432–449.

Bentz, E.C. 2003. Probabilistic Modeling of Service Life for Structures Subjected to Chlorides. *ACI Materials Journal*, Vol. 100, No. 5, pp. 391–397.

Berg, H. P. 2010. Risk Management: Procedures, Methods and Experiences. *Reliability Theory and Applications*, Vol. 1, No. 2, pp. 79–95.

Bertolini, L. 2008. Steel Corrosion and Service Life of Reinforced Concrete Structures. *Structure and Infrastructure Engineering*, Vol. 4, No. 2, pp. 123–137.

Biondini, F., F. Bontempi, D. M. Frangopol, and P. G. Malerba. 2004. Cellular Automata Approach to Durability Analysis of Concrete Structures in Aggressive Environments. *Journal of Structural Engineering*, Vol. 130, No. 11, pp. 1724–1737.

Biondini, F., D. M. Frangopol, and P. G. Malerba. 2008. Uncertainty Effects on Lifetime Structural Performance of Cable-Stayed Bridges. *Probabilistic Engineering Mechanics*, Vol. 23, No. 4, pp. 509–522.

Bocchini, P., D. Saydam, and D. M. Frangopol. 2013. Efficient, Accurate, and Simple Markov Chain Model for the Life-Cycle Analysis of Bridge Groups. *Structural Safety*, Vol. 40, pp. 51–64.

Brehmer, B. and R. Hagafors. 1986. Use of Experts in Complex Judgement Decision Making: A Paradigm for the Study of Staff Work. *Organizational Behaviour and Human Decision Processes*, Vol. 38, No. 2, pp. 181–195.

Brown, P. J. and A. T. Degaetano. 2013. Trends in U.S. Surface Humidity, 1930–2010. *Journal of Applied Meteorology and Climatology*, Vol. 52, pp. 147–163.

Brunswik, E. 1952. *The Conceptual Framework of Psychology*. University of Chicago Press, Chicago, IL.

Bu, G., J. Lee, H. Guan, M. Blumenstein, and Y. C. Loo. 2014. Development of an Integrated Method for Probabilistic Bridge-Deterioration Modeling. *Journal of Performance of Constructed Facilities*, Vol. 28, No. 2, pp. 330–340.

Castro-Borges, P. and J. M. Mendoza-Rangel. 2010. Influence of Climate Change on Concrete Durability in Yucatan Peninsula. *Corrosion Engineering, Science and Technology*, Vol. 45, No. 1, pp. 61–69.

Chen, D. and S. Mahadevan. 2008. Chloride-Induced Reinforcement Corrosion and Concrete Cracking Simulation. *Cement and Concrete Composites*, Vol. 30, No. 3, pp. 227–238.

Choe, D. E., P. Gardoni, D. Rosowsky, and T. Haukaas. 2009. Seismic Fragility Estimates for Reinforced Concrete Bridges Subjected to Corrosion. *Structural Safety*, Vol. 31, No. 4, pp. 275–283.

Dai, A. 2006. Recent Climatology, Variability, and Trends in Global Surface Humidity. *American Meteorological Society*, Vol. 19, pp. 3589–3606.

Delisle, R. R., P. Sullo, and D. A. Grivas. 2004. Element-Level Bridge Deterioration Modeling Using Condition Durations. Transportation Research Board 83th Annual Meeting, January 11–15, Washington, DC.

Dhir, R. K., M. R. Jones, H. E. H. Ahmed, and A. M. G. Seneviratne. 1990. Rapid Estimation of Chloride Diffusion Coefficient in Concrete. *Magazine of Concrete Rese*arch, Vol. 42, No. 152, pp. 177–185.

El Hassan, J., P. Bressolette, A. Chateauneuf, and K. El Tawil. 2010. Reliability-Based Assessment of the Effect of Climatic Conditions on the Corrosion of RC Structures Subject to Chloride Ingress. *Engineering Structures*, Vol. 32, No. 10, pp. 3279–3287.

Fernando, D., Z. Mirzaei, B. T. Adey, and R. M. Ellis. 2012. Identification of More Sustainable Bridge Intervention Strategies. Transportation Research Board 91st Annual Meeting, Washington, DC, January 22–26.

Findlay, S. E. G. and V. R. Kelly. 2011. Emerging Indirect and Long-Term Road Salt Effects on Ecosystems. *Annals of the New York Academy of Sciences*, Vol. 1223, No. 1, pp. 58–68.

Fu, G. and D. Devaraj. 2008. *Methodology of Homogeneous and Non-Homogenous Markov Chains for Modelling Bridge Element Deterioration*. Center for Advanced Bridge Engineering, Wayne State University, Detroit, Michigan.

Funahashi, M. 1990. Predicting Corrosion-Free Service Life of a Concrete Structure in a Chloride Environment. *ACI Materials Journal*, Vol. 87, No. 6, pp. 581–587.

Gaffen, D. J. and R. J. Ross. 1999. Climatology and Trends of U.S. Surface Humidity and Temperature, *Journal of Climate*, Vol. 12, pp. 811–828.

Gigerenzer, G., U. Hoffrage, and H. Kleinbölting. 1991. Probabilistic Mental Models: A Brunswikian Theory of Confidence. *Psychological Review*, Vol. 98, No.4, pp. 506–528.

Gopal, S. and K. Majidzadeh. 1991. Application of Markov Decision Process to Level-of-Service-Based Maintenance System. *Transportation Research Record: Journal of the Transportation Research Board*, No. 1304, pp.12–18.

Han, S-H. 2007. Influence of Diffusion Coefficient on Chloride Ion Penetration of Concrete Structure. *Construction and Building Materials*, Vol. 21, No. 2, pp. 370–378.

Hoffman, P. C. and R. E. Weyers. 1994. Predicting Critical Chloride Levels in Concrete Bridge Decks. *Structural Safety and Reliability*, Vol. 2, pp. 957–959.

Jiang, Y. and K. C. Sinha. 1989. Bridge Service Life Prediction Model Using the Markov Chain. *Transportation Research Record: Journal of the Transportation Research Board*, No. 1223, pp. 24–30.

Khatami, D., B. Shafei, and O. Smadi. 2016. Management of Bridges under Aging Mechanisms and Extreme Events: A Risk-Based Approach. *Transportation Research Record: Journal of the Transportation Research Board*, Vol. 2550, pp. 89–95.

Kirlik, A. 2010. Brunswikian Theory and Method as a Foundation for Simulation-Based Research on Clinical Judgment. *Simulation in Healthcare*, Vol. 5, No. 5, pp. 255–259.
Kobayashi, K, K. Kaito, and N. Lethanh. 2010. Deterioration Forecasting Model with Multistage Weibull Hazard Functions. *Journal of Infrastructure Systems*, Vol. 16, No. 4, pp. 282–291.
Kong, J. S., A. N. Ababneh, D. M. Frangopol, and Y. Xi. 2002. Reliability Analysis of Chloride Penetration in Saturated Concrete. *Probabilistic Engineering Mechanics*, Vol. 17, No. 3, pp. 305–315.
Lee, S. K. 2012. Current State of Bridge Deterioration in the US: Part 1. *NACE International*, Vol. 51, No. 1, pp. 62–67.
Lindell, M. K., and C. S. Prater. 2003. Assessing Community Impacts of Natural Disasters. *Natural Hazards Review*, Vol. 4, No. 4, pp. 176–185.
Lu, S., Y-C. Tu, and H. Lu. 2007. Predictive Condition-Based Maintenance for Continuously Deteriorating Systems. *Quality and Reliability Engineering International*, Vol. 23, pp. 71–81.
Madanat, S. and W. H. W. Ibrahim. 1995. Poisson Regression Models of Infrastructure Transition Probabilities. *Journal of Transportation Engineering*, Vol. 121, No. 3, pp. 267–272.
Martin-Perez, B., S. J. Pantazopoulou, and M. D. A. Thomas. 2001. Numerical Solution of Mass Transport Equations in Concrete Structures. *Computer and Structures*, Vol. 79, No. 3, pp. 1251–1264.
Mauch, M. and S. Madanat. 2001. Semiparametric Hazard Rate Models of Reinforced Concrete Bridge Deck Deterioration. *Journal of Infrastructure Systems*, Vol. 7, No. 2, pp. 49–57.
Mishalani, R. G. and S. M. Madanat. 2002. Computation of Infrastructure Transition Probabilities Using Stochastic Duration Models. *Journal of Infrastructure Systems*, Vol. 8, No. 4, pp. 139–148.
Morcous, G., Z. Lounis, and M. S. Mirza. 2003. Identification of Environmental Categories for Markovian Deterioration Models of Bridge Decks. *Journal of Bridge Engineering*, Vol. 8, No. 6, pp. 353–361.
Morcous, G. 2006. Performance Prediction of Bridge Deck Systems Using Markov Chains. *Journal of Performance Constructed Facilities*, Vol. 20, No. 2, pp. 146–155.
Morcous, G. 2011. Developing Deterioration Models for Nebraska Bridges. Mid-America Transportation Center, University of Nebraska-Lincoln, NE.
Morcous, G. and A. Akhnoukh. 2006. Stochastic Modeling of Infrastructure Deterioration: An Application to Concrete Bridge Decks. Joint International Conference on Computing and Decision Making in Civil and Building Engineering, June 14–16, Montreal, Canada.
IPCC. 2007. *Climate Change 2007: Synthesis Report. Contribution of Working Groups I, II and III to the Fourth Assessment Report of the Intergovernmental Panel on Climate Change*. R. K. Pachauri and A. Reisinger (eds.). Intergovernmental Panel on Climate Change, Geneva, Switzerland.
IPCC. 2014. *Climate Change 2014: Synthesis Report. Contribution of Working Groups I, II and III to the Fifth Assessment Report of the Intergovernmental Panel on Climate Change*. R. K. Pachauri and L. A. Meyer (eds.). Intergovernmental Panel on Climate Change, Geneva, Switzerland.

Papadakis, V. G., A. P. Roumeliotis, M. N. Fardis, C. G. Vagenas. 1996. Mathematical Modeling of Chloride Effect on Concrete Durability and Protection Measures. In *Concrete Repair, Rehabilitation and Protection*. Eds. R. K. Dhir and M. R. Jones. E & FN Spon, London, UK. pp. 165–174.

Ranjith, S., S. Setunge, R. Gravina, and S. Venkatesan. 2013. Deterioration Prediction of Timber Bridge Elements Using the Markov Chain. *Journal of Performance of Constructed Facilities*, Vol. 27, No. 3, pp. 319–325.

Rao, K. B., M. B. Anoop, N. Lakshmanan, S. Gopalakrishnan, and T. V. S. R. A. Rao. 2004. Risk-Based Remaining Life Assessment of Corrosion Affected Reinforced Concrete Structural Members. *Journal of Structural Engineering*, Vol. 31, No. 1, pp. 51–64.

Robelin, C. A. and S. M. Madanat. 2007. History-Development Bridge Deck Maintenance and Replacement Optimization with Markov Decision Processes. *Journal of Infrastructure Systems*, Vol. 13, No. 3, pp. 195–201.

Saetta, A. V., R.V. Scotta, and R.V. Vitaliani. 1993. Analysis of Chloride Diffusion into Partially Saturated Concrete. *ACI Materials Journal*, Vol. 90, No. 5, pp. 441–451.

Scherer, W. T. and D. M. Glagola. 1994. Markovian Models for Bridge Maintenance. *Journal of Transportation Engineering*, Vol. 120, No. 1, pp. 37–51.

Saydam, D., D. M. Frangopol, and Y. Dong. 2013. Assessment of Risk Using Bridge Element Condition Ratings. *Journal of Infrastructure Systems*, Vol. 19, No. 3, pp. 252–265.

Shafei, B., A. Alipour, and M. Shinozuka. 2012. Prediction of Corrosion Initiation in Reinforced Concrete Members Subjected to Environmental Stressors: A Finite Element Framework. *Cement and Concrete Research*, Vol. 42, No. 2, pp. 365–376.

Shafei, B., A. Alipour, and M. Shinozuka. 2013. Stochastic Computational Framework to Investigate the Initial Stage of Corrosion in Reinforced Concrete Superstructures. *Computer-Aided Civil and Infrastructure Engineerin*g, Vol. 28, No. 7, pp. 482–494.

Shafei, B. and A. Alipour. 2015. Estimation of Corrosion Initiation Time in Reinforced Concrete Bridge Columns: How to Incorporate Spatial and Temporal Uncertainties. *Journal of Engineering Mechanics*, Vol. 141, No. 10, pp. 1–12.

Shinozuka, M., M. Q. Feng, H. K. Kim, and S. H. Kim. 2000. Nonlinear Static Procedure for Fragility Curve Development. *Journal of Engineering Mechanics*, Vol. 126, No. 12, pp. 1287–1296.

Simon, J., J. M. Bracci, and P. Gardoni. 2010. Seismic Response and Fragility of Deteriorated Reinforced Concrete Bridges. *Journal of Structural Engineering*, Vol. 136, No. 10, pp. 1273–1281.

Stewart, M. G., and D. V. Rosowsky. 1998. Structural Safety and Serviceability of Concrete Bridges Subject to Corrosion. *Journal of Infrastructure Systems*, Vol. 4, No. 4, pp. 146–155.

Stewart, M. G., X. Wang, and X. Nguyen. 2011. Climate Change Impact and Risks of Concrete Infrastructure Deterioration. *Engineering Structures*, Vol. 33, No. 4, pp. 1326–1337.

Stewart, M. G., X. Wang, and M. N. Nguyen. 2012. Climate Change Adaptation for Corrosion Control of Concrete Infrastructure. *Structural Safety*, Vol. 35, pp. 29–39.

Thompson, P. D., T. Merlo, B. Kerr, A. Cheetham, and R. Ellis. 2000. The New Ontario Bridge Management System. *Presentations for the 8th International Bridge Management Conference*, Transportation Research Circular 498, Vol. 1, pp. F-6/1–F-6/15.

Tsuda, Y., K. Kaito, K. Aoki, and K. Kobayashi. 2006. Estimating Markovian Transition Probabilities for Bridge Deterioration Forecasting. *Structural Engineering/Earthquake Engineering, JSCE*, Vol. 23, No. 2, pp. 241s–256s.

Val, D. and M. G. Stewart. 2003. Life-Cycle Cost Analysis of Reinforced Concrete Structures in Marine Environments. *Structural Safety*, Vol. 25, No. 4, pp. 343–62.

Val, D. V. and P. A. Trapper. 2008. Probabilistic Evaluation of Initiation Time of Chloride-Induced Corrosion. *Reliability Engineering and System Safety*, Vol. 93, No. 3, pp. 364–372.

Wellalage, N. K. W., T. Zhang, and R. Dwight. 2014. Calibrating Markov Chain-Based Deterioration Models for Predicting Future Conditions of Railway Bridge Elements. *Journal of Bridge Engineering*, Vol. 20, No. 2, pp. 1–13.

Xi, Y., Z. P. Bazant, and H. M. Jennings. 1994. Moisture Diffusion in Cementitious Materials. *Advanced Cement Based Materials*, Vol. 1, No. 6, pp. 248–257.

Xi, Y. and Z. P. Bazant. 1999. Modeling Chloride Penetration in Saturated Concrete. *Journal of Materials in Civil Engineering*, Vol. 11, No. 1, pp. 58–65.

Yoon, I., O. Copuroglu, and K. Park. 2007. Effect of Global Climatic Change on Carbonation Progress of Concrete. *Atmospheric Environment*, Vol. 41, No. 34, pp. 7274–7285.

THE INSTITUTE FOR TRANSPORTATION IS THE FOCAL POINT FOR TRANSPORTATION AT IOWA STATE UNIVERSITY.

InTrans centers and programs perform transportation research and provide technology transfer services for government agencies and private companies;

InTrans manages its own education program for transportation students and provides K-12 resources; and

InTrans conducts local, regional, and national transportation services and continuing education programs.

IOWA STATE UNIVERSITY

Visit www.InTrans.iastate.edu for color pdfs of this and other research reports.